U.S. DEPARTMENT OF THE INTERIOR
GEOLOGICAL SURVEY

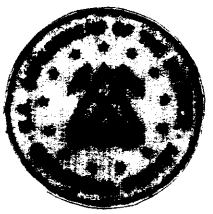

ANALYSIS OF TRACE METALS IN BOTTOM SEDIMENTS IN SUPPORT OF DEEPWATER BIOLOGICAL PROCESSES STUDIES ON THE U.S. NORTH ATLANTIC CONTINENTAL SLOPE AND RISE

By

M. H. Bothner[1], E. Y. Campbell[2], C. M. Parmenter[1], W. Dangelo[2], G. P. DiLisio[1], R. R. Rendigs[1], and J. R. Gillison[2]

Open-File Report 88-2

Final Report
Prepared in cooperation with the
Minerals Management Service
under Interagency Agreement
14-12-0001-30197

[1]Woods Hole, MA
[2]Reston, VA

1987

U.S. DEPARTMENT OF THE INTERIOR
GEOLOGICAL SURVEY

ANALYSIS OF TRACE METALS IN BOTTOM SEDIMENTS IN SUPPORT OF DEEPWATER BIOLOGICAL PROCESSES STUDIES ON THE U.S. NORTH ATLANTIC CONTINENTAL SLOPE AND RISE

By

M. H. Bothner[1], E. Y. Campbell[2], C. M. Parmenter[1], W. Dangelo[2], G. P. DiLisio[1], R. R. Rendigs[1], and J. R. Gillison[2]

Open-File Report 88-2

Prepared in cooperation with the
U.S. Minerals Management Service under
Interagency Agreement No. 14-12-0001-30197

[1]Woods Hole, MA
[2]Reston, VA

1987

CONTENTS

ANALYSIS OF TRACE METALS IN BOTTOM SEDIMENTS IN SUPPORT OF DEEPWATER BIOLOGICAL PROCESSES STUDIES ON THE U.S. NORTH ATLANTIC CONTINENTAL SLOPE AND RISE

FINAL REPORT

M. H. Bothner, E. Y. Campbell, C. M. Parmenter
W. Dangelo, G. P. DiLisio, R. R. Rendigs,
and J. R. Gillison

ABSTRACT

This study is part of a multidisciplinary program conducted on the U.S. continental slope and rise off the North, Middle, and South Atlantic states to characterize the biology, chemistry, and geology of the sea floor in anticipation of exploratory drilling for petroleum resources. The distribution of sediment types and associated trace metals from natural sources will be used to help predict the fate and transport of sediment-reactive contaminants that may be introduced to the water column during future exploration and development activities.

Sediment samples collected during the first three cruises to the continental slope and rise off the North Atlantic states have been analyzed for 12 metals (Al, Ba, Cd, Cr, Cu, Fe, Hg, Mn, Ni, Pb, V, and Zn). The metal concentrations are lower than those reported for world average shales, indicating an absence of major contamination. There is a strong positive correlation between metals and the concentration of silt and clay.

At most locations, slight enrichments of lead (about 30%) were measured in the surface sediments compared to deeper sections of sediment cores. This enrichment is thought to be related to onshore burning of gasoline containing lead additives. Because of our lack of knowledge about the chemical form and bioavailability of lead in these sediments, and because of the lack of similar data in the literature, it is not possible to predict the biological effects of these low-level increases in lead.

Lead-to-aluminum ratios are generally higher in sediments from the axis of Lydonia Canyon than from the adjacent slope. This finding appears to support the hypothesis that increased scavenging of metals from the water column may be occurring in the axis of the canyon as a result of enhanced resuspension of bottom sediment, as documented in a previous study.

INTRODUCTION

This study was designed to establish the concentrations of trace metals in sediments prior to petroleum exploration drilling or other resource development activities on the continental slope and rise off the New England States. This study is part of a cooperative, multidisciplinary program that is managed and funded by the U.S. Minerals Management Service. The overall program objectives are to characterize the slope and rise with respect to benthic infaunal and epifaunal communities, trace-metal and hydrocarbon concentrations in sediments and organisms, sediment texture, and water column hydrography. Separate contracts for major parts of this program have been awarded to Battelle New England Marine Research Laboratory, Woods Hole Oceanographic Institution (WHOI), Lamont-Doherty Geological Observatory, and the U.S. Geological Survey's Branch of Atlantic Marine Geology. Study areas on the continental slope and rise off both the South and Middle Atlantic states are included in the overall program.

The fifteen station locations selected include the major features on the North Atlantic Continental Slope and Rise (Fig. 1). Four stations were established to examine the differences between the axis of Lydonia Canyon and the adjacent continental slope. Two stations were selected to compare environments within and outside of gullies, which are minor topographic features that dissect much of the continental slope. Three stations are just southwest of the new international boundary between the United States and Canada, and may be important in evaluating any effects of future deep drilling conducted by the Canadians. The transect between Stations 11 and 15 is in an area that has been extensively studied during the Shelf Edge Exchange Processes (SEEP) Program funded by the Department of Energy. The two programs complement each other with respect to the types of studies conducted.

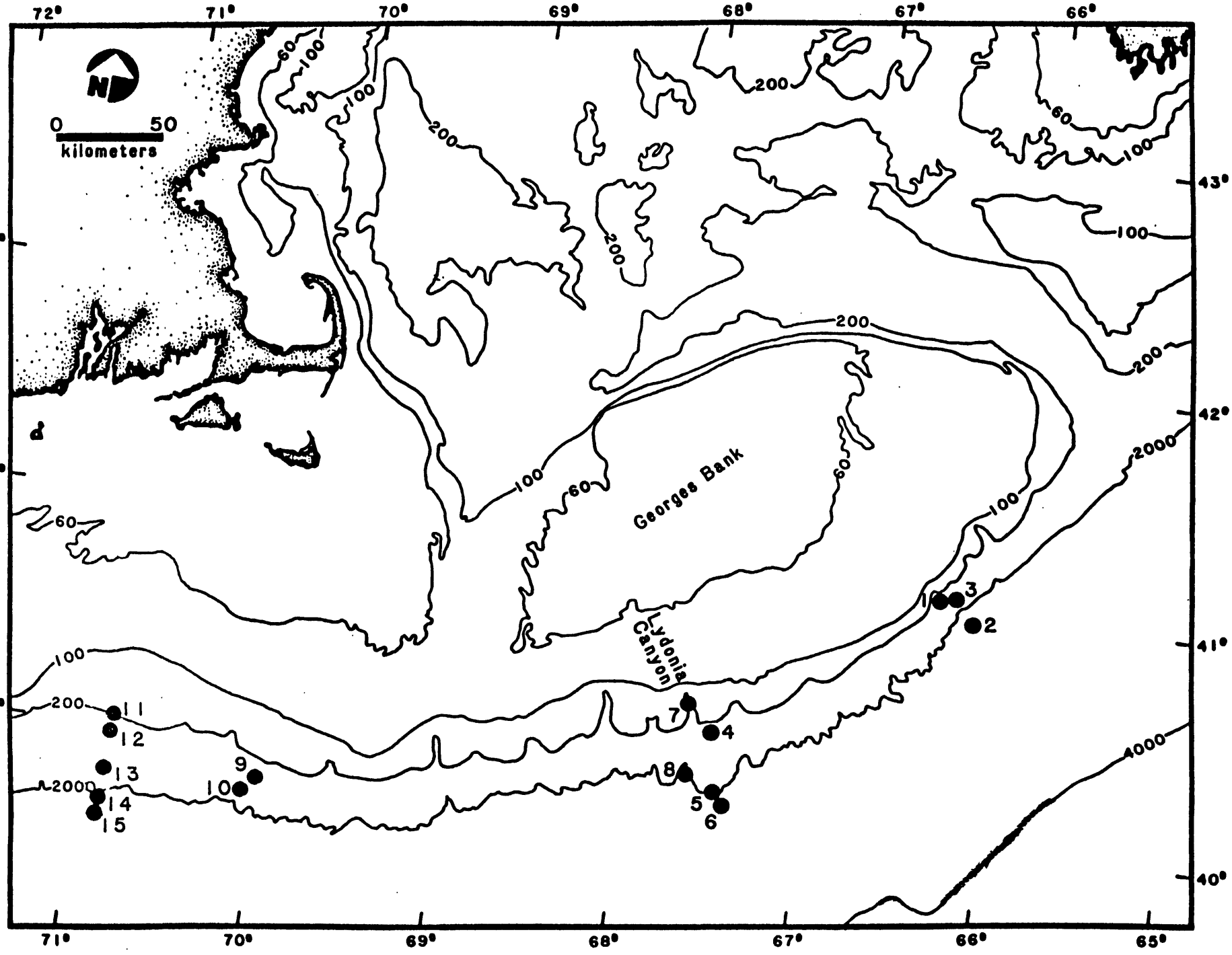

Figure 1. Station locations on the continental slope and rise off the North Atlantic states.

Most of these stations were sampled three times per year for a two-year period. The cruises were conducted in November 1984, April, July, and November 1985, and in April and July, 1986.

FIELD SAMPLING AND SAMPLE PREPARATION

Positioning of the ship at each sampling location was based on time delays within the Loran-C navigation network read by a Northstar 6000 receiver (Digital Marine Equipment Corp., Bedford, Mass.). Latitude and longitude values (Appendix Table 1) were calculated using updated additional secondary factor (asf) corrections (McCullough and others, 1982, 1983). The accuracy of collecting a sample at a given location is more dependent upon wind and current conditions than on the navigation system. Replicate samples collected at a given station typically fall within a circle having a diameter of 400 m.

A 0.25-m^2 box corer, manufactured by Ocean Instruments, Inc., San Diego, Calif., was used to collect sediment samples for this study. The sampling box was divided into 25 subcores of 0.01 m^2 each. Three box cores were collected at each station. Two and occasionally three of the subcores from each box core were allocated for trace-metal studies. Surfaces of the aluminum sub sections were precoated with teflon as a precaution against metal contamination. At sea, an acid-cleaned round plastic tube, 8.2 cm ID, was pushed into the center of the sediments collected in the teflon subcores, thereby sampling material not in contact with the coring apparatus. These tubes were capped at both ends and frozen. The length of the core samples averaged 24 cm and typically ranged from 19 to 32 cm.

Surficial sediment was sampled by partially extruding the frozen sediment from the core barrel and cutting off the top 2 cm of the sediment with a plastic utensil. To generate a blend from a single station, the material from

the upper 2 cm of each of three replicates was thawed, homogenized by stirring and shaking in a closed container, and then subsampled using a syringe constructed of glass and teflon.

On selected samples, sand and coarser material were removed by washing the wet sample through a 60-micron nylon sieve using filtered distilled water. The resultant slurry was dried in an oven having teflon-coated surfaces and a filtered nitrogen atmosphere. Drying temperature for all samples was <70°C.

Cores from selected stations were subsampled in sequential 2-cm depth intervals so that the concentration profiles of metals could be measured over increasing sediment depth. The frozen cores were extruded into a holding tray, thawed overnight, and cut into 2-cm depth intervals with plastic utensils. These samples, from which some of the interstitial water had drained while thawing, were subsequently oven-dried. On the basis of trace metal concentrations in interstitial water reported by Lyons and Fitzgerald, (1983), less than 0.05% of the metal in bulk sediment is lost with the drained interstital water.

All samples prepared for trace-metal analysis were ground using agate grinding tools.

The field numbers (for example, N10123 and N21300) that identify samples in each data table have the following code: the first two characters define the cruise in the North Atlantic region; the second two characters are the station number; the fifth character is the replicate box core number; and the sixth character is the core number within the box core. The use of "00" for the fifth and sixth characters indicates that the sample is a homogenized mixture of subsamples from each of three replicate box cores. Digits in the seventh and eighth space indicate the bottom of a 2-cm-thick depth interval;

where these are missing, the 0-2 cm interval is implied. The letter "X" at the end of the field number indicates that the fraction of sediment coarser than 60 micrometers has been removed from the sample.

TRACE-METAL ANALYSES PROCEDURES

The analyses of trace metals in marine sediments were carried out by the U.S. Geological Survey Branch of Analytical Laboratories, Reston, Va. Concentrations of the following elements were determined: aluminum (Al), barium (Ba), cadmium (Cd), chromium (Cr), copper (Cu), iron (Fe), lead (Pb), manganese (Mn), mercury (Hg), nickel (Ni), vanadium (V), and zinc (Zn). The various procedures employed in each of the analyses are detailed below and summarized in Table 1.

Preparation of stock solution A

Exactly 0.5 g of ground bulk sediment or 0.2 g of the fine fraction was added to a covered teflon beaker and digested overnight at approximately 140°C (hotplate temperature) with 5 mL of $HClO_4$, 5 mL of HNO_3, and 13 mL of HF. The covers were removed and the temperature was increased to between 180° and 190°C, first producing fumes of $HClO_4$ and then evaporating the solution to dryness. The residue was dissolved and diluted to exactly 25 mL with 8 N HCl. This solution is referred to as stock solution A.

Two blanks containing all reagents were analyzed along with samples. All reagents were analyzed for contaminants prior to use, as is always necessary. The Canadian reference sediment standard MESS-1 was analyzed in each set of samples. A series of solutions was prepared that approximated the concentration levels expected in the samples; this series was used as the standard in calibrating the inductively coupled plasma (ICP) spectrometer and atomic absorption (AA) spectrophotometer.

Table 1. Summary of analytical conditions.

Element	Instrument	Instrument conditions	Extraction procedure	Procedure determination limit in sample, µg/g	Average blanks, as measured in µg/g in solution
Al	ICP (argon)	308.2 nm FP (Forward power)=1.1 kw Fixed cross flow nebulizer Spectral band width 0.036 nm Observation height 16 mm.	None	50	0.02
Ba	ICP (argon)	455.4 nm FP=1.1 kw Fixed cross flow nebulizer Spectral band width 0.036 nm Observation height 16 mm.	None	20	.01
Cd	Graphite furnace AA.	110°C dry temperature 250°C char temperature 2100°C atom temperature Regular graphite tube Interrupt gas flow W.l.=228.8 nm Slit=0.7 nm.	Butyl acetate and DDTC.	0.02	.0002
Cr	Graphite furnace AA.	110°C dry temperature 850°C char temperature 2700°C atom temperature Pyrolitic tube Normal gas flow (low) W.l.=357.9 nm Slit=0.7 nm.	None	2	.003
Cu	Graphite furnace AA.	110°C dry temperature 900°C char temperature 2700°C atom temperature Regular graphite tube Interrupt gas flow W.l.=324.7 nm Slit=0.7 nm.	Butyl acetate and DDTC.	1	.005
Fe	ICP (argon)	259.9 nm FP=1.1 kw Fixed cross flow nebulizer Spectral band width 0.036 nm Observation height 16 nm.	None	50	.02
Hg	Induction furnace AA.	Wavelength=254 nm Cold vapor AA.	None	.005	.005
Mn	ICP (argon)	257.6 nm FP=1.1 kw Fixed cross flow nebulizer Spectral band width 0.036 nm Observation height 16 nm.	Butyl acetate (removal of iron).	10	.006
Ni	Graphite furnace AA.	110°C dry temperature 900°C char temperature 2700°C atom temperature Pyrolytic tube Normal gas flow (low) W.l.=232.0 nm Slit=0.2 nm.	None	2	.02
Pb	Graphite furnace AA.	110°C dry temperature 500°C char temperature 2700°C atom temperature Regular graphite tube Interrupt gas flow W.l.=283.3 Slit=0.7 nm.	Butyl acetate and DDTC.	1	.02
V	Graphite furnace AA.	110°C dry temperature 1000°C char temperature 2800°C atom temperature Pyrolytic curtained tube Normal gas flow (high) W.l.=318.4 nm Slit=0.7 nm.	None	2	.002
Zn	Flame AA.	Oxidizing; air-acetylene flame W.l.=213.9 Slit=0.7 nm.	Butyl acetate	1	.01

Preparation of stock solution B

Stock solution B was made by adding 10 mL of butyl acetate (distilled to remove impurities such as copper) to 15 mL of stock solution A in a 60-mL separatory funnel. This solution was vigorously agitated by an automatic shaker for six minutes to extract iron. The layers were separated, and the extraction step was repeated with an additional 10 mL of butyl acetate. The aqueous layer was evaporated to dryness at 150°C in a 50-mL beaker. The residue was dissolved and diluted to 25 mL with 1 N HCl.

Barium

The measurements for Ba were made by ICP spectrometry with 2 mL of stock solution A diluted to 4 mL with distilled H_2O.

Aluminum, iron, chromium, nickel, and vanadium

Concentrations of Al and Fe were determined by ICP spectrometry by using 1 mL of stock solution A diluted to 10 mL with distilled H_2O. The measurements for Cr, Ni, and V were made by injecting 20 µL of diluted (1:10) stock solution A into a graphite-furnace AA spectrophotometer.

Lead, copper, and cadmium

Fifteen mL of 0.5-percent (weight:volume) diethyldithiocarbamic acid diethylammonium salt (DDTC) in chloroform were added to 10 mL of solution B in a 60-mL separatory funnel and mixed for 10 minutes by an automatic shaker. The chloroform layer was drained into a 30-mL beaker and the aqueous layer washed with 10 mL of chloroform. The second chloroform layer was combined with the first, and the total volume of chloroform was evaporated to dryness at 90°C. The organic matter was destroyed by adding 0.1 mL of concentrated HNO_3 and was evaporated to dryness. This residue then was dissolved in 2 mL of warm 1 N HCl. The beaker was rinsed four times with 2 mL portions of distilled H_2O, and the solution was transferred to a small polyethylene

container. The measurements for Pb, Cu, and Cd were made by injecting 20 µL of the final solution into a graphite-furnace AA spectrophotometer.

Manganese and zinc

The measurements for Mn were made by ICP spectrometry using a solution made by diluting 2 mL of stock solution B to 4 mL with H_2O. Zinc was measured by flame AA directly from stock solution B.

Mercury

Mercury concentration was determined on a separate portion of the sample. Two hundred milligrams of sediment were decomposed in a 1-oz teflon screw-top vial containing 2 mL of concentrated HNO_3 (J. T. Baker Chemical Co.) and 2 mL of $HClO_4$ (G. Frederick Smith Chemical Co. (GFS) double distilled from Vycor, a pure silica glass). The mixture was heated in a capped vial until the solution reached 200°C. The solution was then heated with the cap off for about 45 minutes, after which the samples were removed from the heat source. Immediately, 1 mL of concentrated HNO_3 was added; the vial was filled with H_2O and capped tightly until used. The sample solution then was added to a flask containing 125 mL of H_2O and 4 mL of 10-percent (weight:volume) $SnCl_2$ in 20% HCl. Nitrogen was passed through the solution to remove elemental Hg, which was collected on gold foil located in the center of the coils of an induction furnace. Activation of the furnace released the Hg, which was measured by a cold-vapor AA technique. Blanks, standard rocks, and internal sediment standards were analyzed for each set of samples. A series of solutions was prepared that had the same Hg concentration range expected in the samples.

ANALYTICAL ACCURACY AND PRECISION

Analytical accuracy was determined by analyzing rock standard MESS-1. All of the metals are within one or, at most, two standard deviations of the "best value" determined for this sediment standard (Table 2). A new fine-grained sediment standard (B series, Table 2) established for the Georges Bank Monitoring Program (Bothner and others, 1985b) was also used during this program.

Analytical precision was determined by periodically analyzing replicate aliquots taken from a single sample. Coefficients of variation shown in Table 2 indicate that the standard deviations are typically less than 10 percent of the mean value, except for Cd and Ni determinations at concentrations less than five times the detection limit.

During the early phases of this program, we evaluated the metal concentrations in surface sediments that were in contact with different materials used in the box of the box corer (Bothner and others, 1985a). In the bulk sediments, vanadium values may be slightly higher in the samples collected from the edge of the teflon-coated subcore than in the other samples. In the fine fraction, the lead values from the edges of the subcores are about 40 percent higher than in the sediment not in contact with the box-core material.

The material collected at the edges of the subcore probably represent the worst case for contamination from the material used to construct the box-core sample chamber. The sediment that is routinely removed from the subcore for trace-metal analysis excludes the material in contact with the wall of the subcore. We therefore conclude that contamination from the walls of the box core is insignificant. This test does not rule out the possibility that metal contamination could occur from flakes of material falling onto the sediment

Table 2. - Analysis of sediment standard and replicate sediment samples.

Sediment standard	Al (%)	Ba (ppm)	Cd (ppm)	Cr (ppm)	Cu (ppm)	Fe (%)	Hg (ppm)	Mn (ppm)	Ni (ppm)	Pb (ppm)	V (ppm)	Zn (ppm)
MESS-1	4.89	259	0.42	60	25	2.80	0.14	483	31	25	80	178
	5.06	259	.41	61	28	2.85	.14	489	34	27	74	186
	5.16	266	.42	61	24	2.84		491	36	22	88	173
	4.64	266	.39	61	23	2.77		492	36	26	78	178
	5.41	258	.48	65	23	2.78		469	35	31	85	174
$\bar{x}$	5.03	262	.42	61.8	24.6	2.81	.14	485	34.4	26.2	81	178
σ	.29	4	.03	1.8	2.11	.04		9.5	2.11	3.3	5.6	5.1
CV(%)[1]	5.7	1.5	7.9	2.9	8.4	1.3		2	6	12	6.9	2.9
Best value[2]	5.8	261	.59	71	25	3.0		513	30	34	72	191
σ	.2	18	.1	11	4	.2		25	3	6	5	17

Sediment standard	Al (%)	Ba (ppm)	Cd (ppm)	Cr (ppm)	Cu (ppm)	Fe (%)	Hg (ppm)	Mn (ppm)	Ni (ppm)	Pb (ppm)	V (ppm)	Zn (ppm)
B-11[3]	3.26	258	.080	47	6.5	1.63	.014	292	14	13	46	40
	3.33	269	.075	42	5.6	1.62	.015	285	13	15	44	40
	3.45	265	.075	46	5.9	1.60		286	9.5	15	44	36
$\bar{x}$	3.35	264	.077	45	6	1.62	.0145	288	12.2	14.3	44.7	38.7
σ	.1	5.6	.003	2.6	.5	.01	.0007	3.8	2.4	1.2	1.2	2.3
CV(%)[1]	2.9	2.1	3.7	5.9	7.6	.9	4.9	1.3	19	8	2.6	5.9

Sediment sample	Al (%)	Ba (ppm)	Cd (ppm)	Cr (ppm)	Cu (ppm)	Fe (%)	Hg (ppm)	Mn (ppm)	Ni (ppm)	Pb (ppm)	V (ppm)	Zn (ppm)
N1061104	4.26	338	.075	61	13	2.21	.005	295	24	8.3	58	49
W-230741	4.28	334	.075	63	13	2.21	.005	305	24	8.8	58	48
	4.27	336	.083	61	13	2.20	.005	298	24	8.3	62	48
	4.38	333	.095	63	14	2.25	.005	299	24	9.5	60	49
	4.32	331	.095	63	14	2.23	.005	305	24	9.5	62	49
$\bar{x}$	4.30	334	.085	62.2	13.4	2.22	.005	300	24	8.9	60	48.6
σ	.05	27	.01	1.1	.5	.02	0	4.4	0	.6	2	.5
CV(%)[1]	1.1	.8	12	1.8	4.1	.9	0	1.5	0	6.7	3.3	1.1

Sediment sample	Al (%)	Ba (ppm)	Cd (ppm)	Cr (ppm)	Cu (ppm)	Fe (%)	Hg (ppm)	Mn (ppm)	Ni (ppm)	Pb (ppm)	V (ppm)	Zn (ppm)
N2040002	2.44	208	<.02	33	4.6	1.58	.006	269	6.5	55	35	22
W-232076	2.43	208	<.02	33	5.0	1.56	.005	268	5.0	5.8	38	23
	2.44	209	<.02	29	5.6	1.53	.005	269	6.5	5.5	35	25
	2.41	207	<.02	34	4.6	1.54	.005	269	5.0	2.8	40	22
	2.43	208	<.02	34	5.3	1.58	.005	270	6.5	5.8	40	23
$\bar{x}$	2.43	208	<.02	32.6	5.0	1.56	.0052	269	5.9	5.68	37.6	23
σ	.01	.7		2.1	.4	.02	.004	.7	.8	.16	2.5	1.2
CV(%)[1]	.5	.3		6.4	8.7	1.5	8.6	.3	14	2.9	6.7	5.3

Sediment sample	Al (%)	Ba (ppm)	Cd (ppm)	Cr (ppm)	Cu (ppm)	Fe (%)	Hg (ppm)	Mn (ppm)	Ni (ppm)	Pb (ppm)	V (ppm)	Zn (ppm)
N3020002	5.04	420	.050	68	21	2.89		782	34	13	87	73
W-232048	5.03	421	.046	71	23	2.90		768	36	11	94	73
	4.98	419	.055	68	21	2.86		771	34	12	87	73
	4.97	420	.055	66	22	2.88		775	33	12	87	73
	4.98	417	.050	66	23	2.87		766	35	12	94	73
$\bar{x}$	5.0	419	.051	67.8	22	2.88		772	34.4	12	89.8	73
σ	.03	1.5	.004	2	1	.02		6.3	1.1	.7	3.8	0
CV(%)[1]	.6	.4	7.5	3	4.5	.5		.8	3.3	2	4.3	0

[1]Coefficient of variation.
[2]Values reported by the Marine Analytical Chemistry Standards Program, National Research Council, Canada.
[3]A fine-grained sediment standard collected from station 13 of the Georges Bank Monitoring Program (Bothner and others, 1983).

surface from the coring apparatus above the sample box, but such contamination would be random and severe and should be obvious from the analytical results. Within this program we have observed less than ten spurious values that might be explained by contamination from field or laboratory operations.

RESULTS AND DISCUSSION

Within-station variability

We determined the variability of metal concentrations within an individual box core and between replicate box cores taken at the same station (Table 3A-B).

At Station 4 the average within-box core variability is 9.6 %, and the average within-station variability is 15 %. At station 7, where the average within-station variability is 19% (table 3B), the rank order of aluminum concentrations among replicates is identical to the rank order of clay concentrations (Battelle and others, 1986). Aluminum is commonly used as an indicator for the content of fine-grained sediments and the strong correlation suggests that the within-station (and probably the within-box core) variability is simply related to texture.

The variability in metals at stations 4 and 7 is higher than measured at station 1 in the Mid-Atlantic study area (7.2% within-box core variability, 8% within-station variability; Bothner and others, 1986). The texture at stations 4 and 7 is coarser and the variability in the percentage of clay is greater than station 1 in the Mid-Atlantic study area. For example, the clay content varies by a factor of 2 within some of the replicates at station 4 (Battelle and others, 1986).

Small-scale variability in texture on the sediment surface, has been observed from the submersible ALVIN in the North Atlantic study area

Table 3A. - Comparison of within-station variability to within-box-core variability at Station 4, Cruises 1, 2, 3; and at Stations 6 and 8, Cruise 5.

Field no.	Top (cm)	Btm (cm)	Lab no.	Al (%)	Ba (ppm)	Cd (ppm)	Cr (ppm)	Cu (ppm)	Fe (%)	Hg (ppm)	Mn (ppm)	Ni (ppm)	Pb (ppm)	V (ppm)	Zn (ppm)
N10411	0	2	W-230145	2.69	239	<0.020	38	9.8	1.73	0.01	292	7.0	9.1	33	27
N10421	0	2	W-230146	2.50	240	<.020	36	4.0	1.46	.01	255	6.0	7.1	33	23
N10431	0	2	W-230147	2.34	218	<.020	34	3.0	1.43	.01	238	3.0	6.3	33	23
$\bar{x}$				2.51	232		36	5.6	1.54	.01	262	5.3	7.5	33	24.3
σ				.17	12		2.0	3.7	.16	0	28	2.1	1.4	0	2.3
CV%[1]				7.0	5.3		5.6	66	11	0	10	39	19	0	9.5
N10431	0	2	W-230147	2.34	218	<.020	34	3.0	1.43	.01	238	3.0	6.3	33	23
N10432	0	2	W-230148	2.29	212	<.020	33	3.2	1.46	.01	230	3.0	6.6	25	23
N10433	0	2	W-230149	2.36	219	<.033	34	3.2	1.46	.01	249	3.0	6.6	26	27
$\bar{x}$				2.33	216		33.7	3.1	1.45	.01	239	3	6.5	28	24.3
σ				.04	3.8		.6	.1	.02	0	9.5	0	.2	4.4	2.3
CV%[1]				1.5	1.8		1.7	3.7	1.2	0	4.0	0	2.7	16	9.5
N20411	0	2	W-232088	2.77	214	<.020	44	5.0	1.80	.01	308	6.5	6.0	38	22
N20421	0	2	W-232091	2.36	208	<.020	32	4.6	1.44	.01	295	3.0	6.6	38	20
N20431	0	2	W-232092	2.37	213	.025	32	4.0	1.52	<.01	272	6.5	6.0	40	18
$\bar{x}$				2.5	212		36	4.5	1.59		292	5.3	6.2	38.7	20
σ				.23	3.2		6.9	.5	.19		18	2.0	.3	1.2	2.0
CV%[1]				9.4	1.5		19	11	12		6.2	38	5.6	3	10
N20411	0	2	W-232088	2.77	214	<.020	44	5.0	1.80	.01	308	6.5	6.0	38	22
N20412	0	2	W-232089	2.66	218	<.020	36	4.0	1.74	.01	313	8.0	7.1	52	25
N20413	0	2	W-232090	2.60	220	.360	36	4.6	1.65	<.01	294	3.0	6.6	40	22
$\bar{x}$				2.68	217		38.7	4.5	1.73		305	5.8	6.6	43.3	23
σ				.09	3.1		4.6	.5	.07		9.8	2.6	.6	7.6	1.7
CV%[1]				3.2	1.4		12	11	4.4		3.2	44	8.3	17	7.5
N30411	0	2	W-232054	2.41	199	.022	36	4.2	1.60	.01	287	8.0	6.3	22	25
N30421	0	2	W-232057	2.84	203	.170	43	5.3	1.83	.01	277	12	7.1	28	28
N30431	0	2	W-232058	2.20	190	.055	33	4.3	1.50	.01	253	10	6.3	<2.0	17
$\bar{x}$				2.48	197	.082	37.3	4.6	1.64	.01	272	10	6.6		23.3
σ				.33	6.6	.078	5.1	.6	.17	0	17	2	.5		5.7
CV%[1]				13	3.4	94	14	13	10	0	6.4	20	7.0		24
N30411	0	2	W-232054	2.41	199	.022	36	4.2	1.60	.01	287	8.0	6.3	22	25
N30412	0	2	W-232055	2.46	199	.080	48	4.0	1.62	.01	254	8.0	7.5	17	22
N30413	0	2	W-232056	2.87	232	.055	42	7.5	1.84	.01	285	12	6.3	28	28
$\bar{x}$				2.58	210	.052	42	5.2	1.69	.01	275	9.3	6.7	22.3	25
σ				.25	19	.029	6.0	2.0	.13	0	18	2.3	.7	5.5	3
CV%[1]				9.8	9.1	56	14	38	7.9	0	6.7	25	10	25	12

Table 3A. - Continued - Comparison of within-station variability to within-box-core variability at Stations 6 and 8, Cruise 5.

Field no.	Top (cm)	Btm (cm)	Lab no.	Al (%)	Ba (ppm)	Cd (ppm)	Cr (ppm)	Cu (ppm)	Fe (%)	Hg (ppm)	Mn (ppm)	Ni (ppm)	Pb (ppm)	V (ppm)	Zn (ppm)
N50611	0	2	W-236894	3.19	263	.043	45	14	1.65	.00	437	19	10.0	56	46
N50612	0	2	W-236902	3.13	263	.063	47	13	1.64	.00	461	18	10.0	60	42
N50613	0	2	W-236903	3.03	249	.057	46	13	1.60	.00	430	20	10.0	54	31
$\bar{x}$				3.12	258	.054	46.0	13.33	1.63	.005	442.7	19.0	10.0	56.7	39.7
σ				0.08	8.1	.010	1.0	.58	.062	.000	16.3	1.0	.0	3.1	7.8
CV%[1]				2.59	3.1	19.0	2.2	4.3	1.59	0.	3.7	5.3	0.	5.4	19.6
N50611	0	2	W-236894	3.19	263	.043	45	14	1.65	.00	437	19	10.0	56	46
N50621	0	2	W-236895	2.89	248	.022	45	15	1.56	.00	456	16	11.0	46	34
N50631	0	2	W-236896	3.09	256	.033	50	15	1.68	.00	470	19	7.1	60	39
$\bar{x}$				3.057	255.7	.0327	46.7	14.7	1.63	.005	454.3	18.0	9.37	54.0	39.7
σ				0.153	7.5	.0105	2.89	0.58	.062	.000	16.56	1.73	2.03	7.21	6.03
CV%[1]				5.00	2.94	32.11	6.19	1.24	0.43	-	3.65	9.61	21.67	13.35	15.24
N50811	0	2	W-236897	3.51	301	.0201	56	14	1.96	.01	486	22	13.0	65	98
N50821	0	2	W-236898	3.34	286	.035	55	19	1.89	.01	387	19	17.0	66	54
N50831	0	2	W-236899	3.67	299	.050	63	18	2.02	.01	498	25	21.0	75	74
$\bar{x}$				3.507	295.3	.035	58.0	17.0	1.96	.009	457.0	22.0	17.0	68.67	75.33
σ				0.165	8.14	.015	4.36	2.65	.065	.011	60.92	3.00	4.0	5.51	22.03
CV%[1]				4.70	2.76	42.86	7.52	15.59	3.32	11.83	13.33	13.64	23.53	8.02	29.24
N50811	0	2	W-236897	3.51	301	.0201	56	14	1.96	.01	486	22	13.0	65	98
N50812	0	2	W-236900	3.25	291	.037	52	16	1.83	.01	425	19	13.0	64	52
N50813	0	2	W-236901	3.42	288	.022	56	16	1.91	.01	431	25	14.0	66	44
$\bar{x}$				3.39	293.33	.026	54.7	15.3	1.90	.01	447.3	22.0	13.3	65.00	64.67
σ				0.132	6.81	.009	2.31	1.15	.066	.00	33.62	3.00	0.58	1.00	29.14
CV%[1]				3.89	2.32	35.36	4.23	7.50	3.47	.00	7.51	13.64	4.35	1.54	45.06

Table 3B. - Within-station variability at Station 7, (axis of Lydonia Canyon), Cruises 1, 2, 3.

Field no.	Top (cm)	Btm (cm)	Lab no.	Al (%)	Ba (ppm)	Cd (ppm)	Cr (ppm)	Cu (ppm)	Fe (%)	Hg (ppm)	Mn (ppm)	Ni (ppm)	Pb (ppm)	V (ppm)	Zn (ppm)
N10711	0	2	W-230150	2.09	174	0.030	48	5.3	2.55	0.01	211	8.0	11	33	30
N10721	0	2	W-230151	1.56	152	.021	45	2.0	2.50	.01	188	<2.0	7.1	28	23
N10731	0	2	W-230152	1.73	175	.033	43	4.5	1.98	.01	230	<2.0	7.1	33	25
$\bar{x}$				1.79	167	.028	45.3	3.9	2.34	.01	210		8.4	31.3	26
σ				.27	13	.006	2.5	1.7	.32	0	21		2.2	2.9	3.6
CV%[1]				15	7.8	22	5.5	44	13	0	10		27	9.2	14
N20711	0	2	W-232093	1.61	157	<.020	38	3.3	2.18	<.01	182	3.0	6.0	38	17
N20721	0	2	W-232094	1.36	148	<.020	28	3.3	1.75	<.01	197	3.0	6.0	21	1.3
N20731	0	2	W-232095	1.04	106	<.020	36	<1.0	2.44	.01	128	<2.0	6.0	15	<1.0
$\bar{x}$				1.34	137		34		2.12		169		6.0	24.7	
σ				.29	27		5.3		.35		36		0	11.9	
CV%[1]				21	20		16		16		21		0	48	
N30711	0	2	W-232059	1.63	148	.033	45	4.3	2.42	.01	213	7.0	7.1	25	20
N30721	0	2	W-232060	1.52	136	.025	46	3.8	3.10	.01	225	4.0	6.3	17	23
N30731	0	2	W-232061	2.18	205	.066	62	8.0	3.04	.01	204	10	6.6	34	27
$\bar{x}$				1.78	163	.041	51	5.4	2.85	.01	214	7	6.7	25.3	23.3
σ				.35	37	.021	9.5	2.3	.38	0	10	3	.4	8.5	3.5
CV%[1]				20	23	53	19	43	13	0	4.9	43	6.0	34	15

(Valentine and others, 1980). Some of this variability has been attributed to ice rafting during glacial periods. This geologic process, more active in northern latitudes, might account for the higher within-station variability in texture and in metals than that observed at stations in the Mid-Atlantic area.

Distribution of metals in surface sediments

The distribution of metals in surface sediments of the continental slope appears to be strongly influenced by the distribution of fine sediments. The correlation is graphically shown in Figures 2A, 2B, and 2C (data from Table 4). Except for Cd (often near the limit of detection), the concentrations of metals and clay are very similar from station to station. Specifically, the concentrations of clay and most of the metals are higher at Station 2 than those at adjacent stations (Fig. 2A-2C). At stations 5, 7, and 11, we observed the lowest concentrations of clay and most of the metals.

To test the relationship between fine sediments and metals we used nylon sieves to separate two sediment samples into sequential grain size classes and analyzed each fraction for metals. Generally there is an increase in metal concentration with decreasing sediment size (Table 5). Exceptions to this trend are the exceptionally high concentrations of Fe and Mn in the sand fraction from station 7, which could be due to precipitation of these metals in the surface sediments.

Additional but less detailed evidence that the finest sediment fractions contain the highest concentrations of metals is presented in Table 6. The sediment fraction finer than 60 μm and between 10-30 μm are typically a factor of 2 higher than concentrations in the bulk sample (Table 4).

The concentrations of metals in sediments analyzed in this study are the same or lower than the concentrations of metals reported by Krauskopf (1967) in average shales from various locations around the world. This similarity

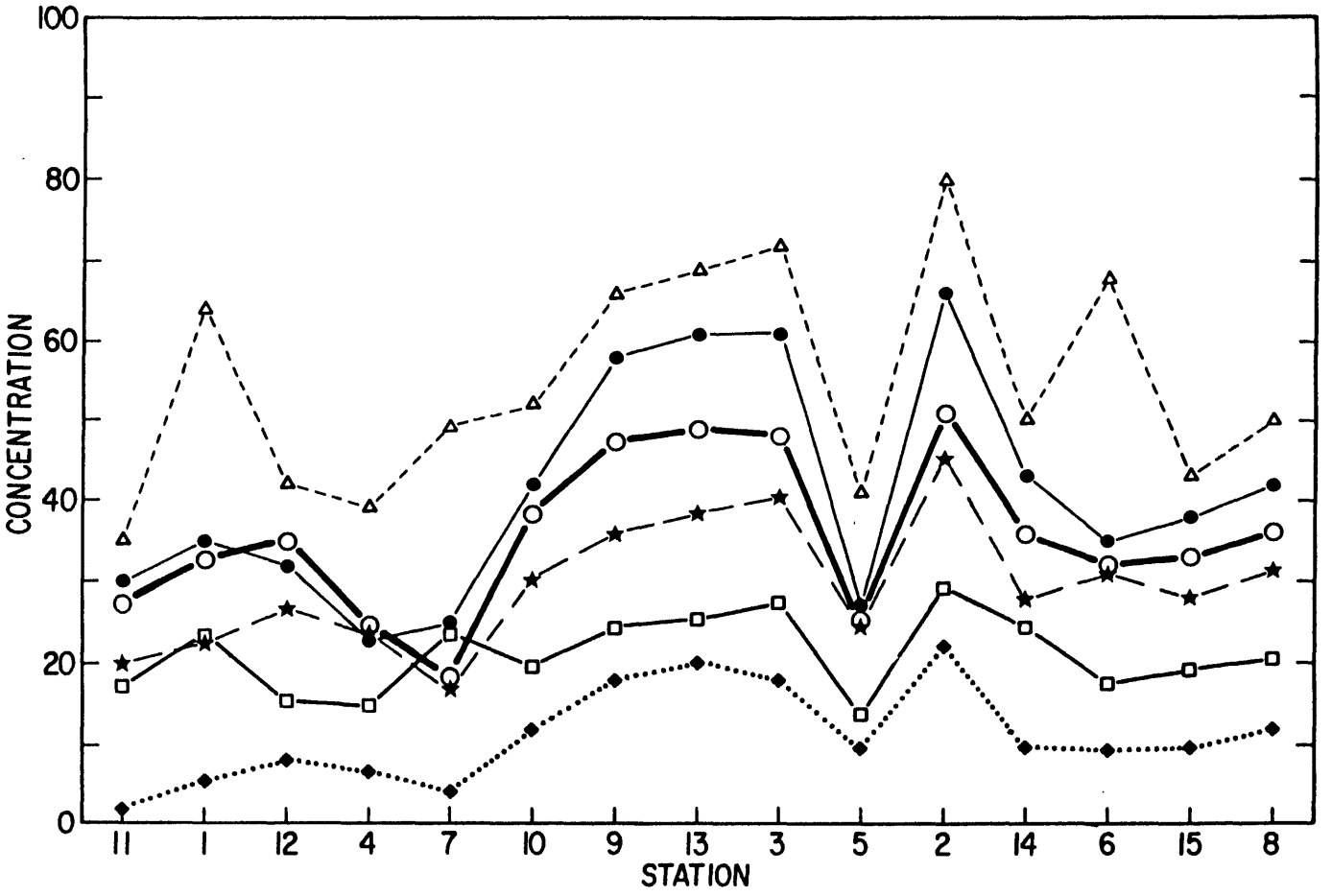

Figure 2A. Concentrations of metals in station blends for Cruise 1. Stations listed from shallowest to deepest. (Al, ○ % x 10; Ba, ★ ppm x 10^{-1}; Cr, △ ppm; Cu, ◆ ppm; Fe, □ % x 10; Zn, ● ppm.)

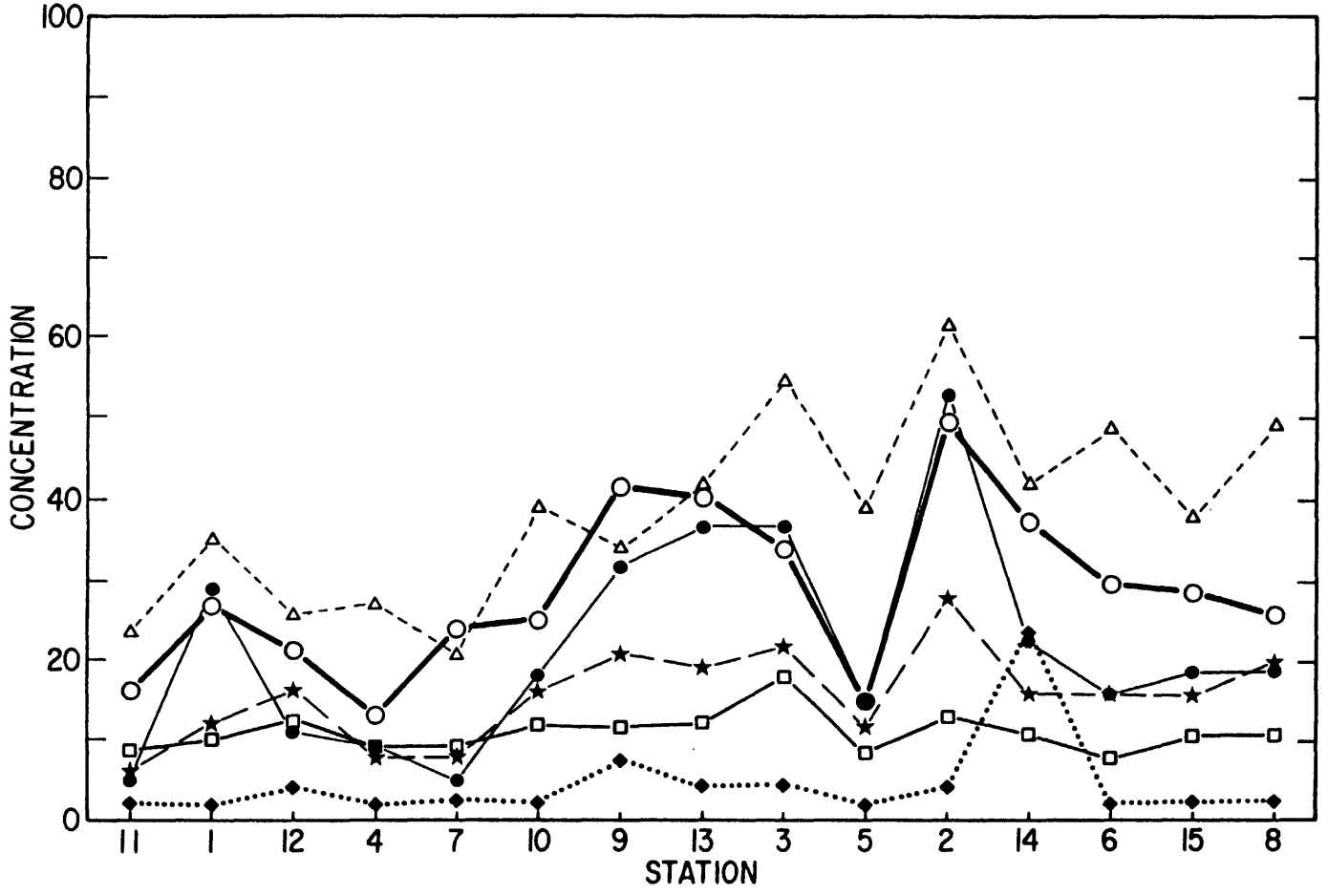

Figure 2B. Concentrations of metals in station blends from Cruise 1. Stations listed from shallowest to deepest. (Cd, ◆ ppm x 10^2; Hg, ★ ppm x 10^2; Mn, △ ppm x 10^{-1}; Ni, ● ppm; Pb, □ ppm; V, ○ ppm x $\frac{1}{2}$.)

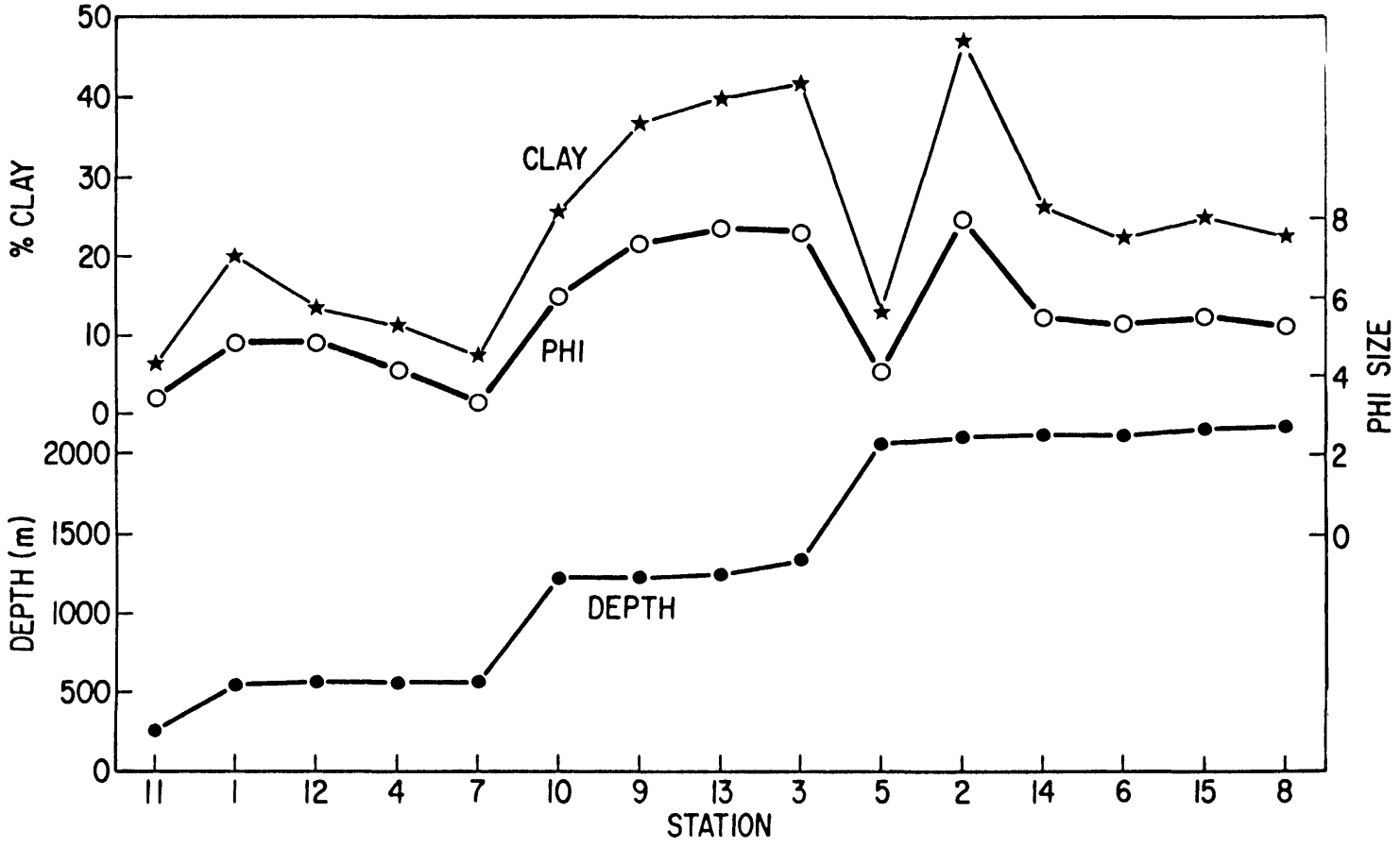

Figure 2C. Average concentration of clay (★ in percent), mean grain size (○) in phi units ($-\log_2 D$, where D = grain diameter in mm), and water depth (● in meters) at stations from Cruise 1 listed from shallowest to deepest.

Table 4. - Chemical Analysis of station blends.

Field no.	Top (cm)	Btm (cm)	Lab no.	Al (%)	Ba (ppm)	Cd (ppm)	Cr (ppm)	Cu (ppm)	Fe (%)	Hg (ppm)	Mn (ppm)	Ni (ppm)	Pb (ppm)	V (ppm)	Zn (ppm)
N10100	0	2	W-230130	3.27	224	<.020	64	5.5	2.33	.01	354	29	10	54	35
N10200	0	2	W-230131	5.10	453	.042	80	22	2.91	.03	617	53	13	99	66
N20200	0	2	W-232074	5.00	431	.046	65	22	2.84	.03	919	38	12	134	70
N30200	0	2	W-232048	5.00	419	.051	68	22	2.88	.01	772	34	12	90	73
N40200	0	2	W-234553	4.78	416	.025	74	22	2.75	.02	696	52	16	84	65
N50200	0	2	W-236884	5.06	389	.110	77	29	2.87	.02	486	50	31	82	900?
N60200	0	2	W-237752	4.77	398	.054	74	28	2.71	.03	696	40	18	100	79
N10300	0	2	W-230132	4.80	404	.042	72	18	2.73	.02	548	37	18	68	61
N20300	0	2	W-232075	4.56	371	.025	63	17	2.56	.02	641	30	12	117	58
N30300	0	2	W-232049	4.59	358	.055	63	18	2.66	.04	740	29	15	87	68
N40300	0	2	W-234554	4.69	378	.046	72	18	2.62	.02	582	48	16	93	63
N50300	0	2	W-236885	4.50	325	.110	66	23	2.48	.01	519	32	26	72	66
N60300	0	2	W-237753	4.01	364	.033	63	17	2.19	.03	485	28	19	79	52
N10400	0	2	W-230133	2.45	236	<.020	39	6.3	1.48	.01	271	9.0	9.1	26	23
N20400	0	2	W-232076	2.43	208	<.020	33	5.0	1.56	.01	269	5.9	5.7	38	23
N30400	0	2	W-232050	2.45	197	.025	36	5.6	1.61	.02	263	8.0	6.3	20	23
N10500	0	2	W-230134	2.52	248	.021	41	9.8	1.38	.01	395	15	8.8	30	27
N20500	0	2	W-232077	2.60	244	.025	34	6.1	1.33	.01	407	8.0	5.5	38	22
N30500	0	2	W-232051	2.64	231	.030	40	7.5	1.41	.02	403	12	4.6	10	25
N40500	0	2	W-234555	2.84	264	<.020	46	9.6	1.55	.01	432	23	11	39	32
N50500	0	2	W-236886	2.52	206	.040	38	11	1.38	.00	414	14	8.7	36	35
N60500	0	2	W-237754	2.55	229	.028	37	9.6	1.39	.01	369	13	8.3	42	29
N10600	0	2	W-230135	3.21	307	.021	68	9.3	1.74	.02	491	16	8.0	59	35
N20600	0	2	W-232078	3.23	284	<.020	41	9.6	1.68	.02	446	14	5.5	78	27
N40600	0	2	W-234556	3.11	289	.025	45	9.8	1.70	.02	466	20	9.6	44	37
N50600	0	2	W-236887	3.05	251	<.020	44	14	1.61	.00	439	19	10.0	48	39
N60600	0	2	W-237755	3.03	268	<.020	48	13	1.75	.02	451	18	11.0	58	32
N10700	0	2	W-230136	1.84	167	.025	49	4.0	2.36	.01	206	5.0	9.1	47	25
N20700	0	2	W-232079	1.31	132	<.020	35	<1.0	2.15	<.01	162	<2.0	5.5	15	<1.0
N30700	0	2	W-232052	.80	140	.055	52	5.3	2.77	.01	218	7.0	8.8	22	25
N10800	0	2	W-230137	3.60	312	.025	50	12	2.05	.02	492	19	11	52	42
N20800	0	2	W-232080	3.15	296	<.020	47	9.0	1.79	.02	457	16	7.6	49	35
N30800	0	2	W-232053	2.86	275	.030	44	10	1.66	.02	367	12	7.5	40	32
N40800	0	2	W-234557	3.38	470	.040	55	11	2.00	.01	385	28	11	51	38
N50800	0	2	W-236888	3.42	298	.038	55	16	1.91	.01	448	20	15	62	68
N60800	0	2	W-237756	2.33	210	.028	37	8	1.52	.01	280	12	9.8	39	23
N10900	0	2	W-230138	4.72	359	.075	66	18	2.44	.02	343	32	12	83	58
N20900	0	2	W-232081	4.54	343	.037	61	14	2.40	.03	530	28	11	106	61
N40900	0	2	W-234558	4.44	337	.096	72	19	2.27	.02	424	43	11	84	58
N50900	0	2	W-236889	4.73	326	.150	71	23	2.48	.01	321	52	17	94	400?
N60900	0	2	W-237757	4.14	296	.076	73	16	2.38	.03	362	31	15	92	63

Table 4 - Continued

Field no.	Top (cm)	Btm (cm)	Lab no.	Al (%)	Ba (ppm)	Cd (ppm)	Cr (ppm)	Cu (ppm)	Fe (%)	Hg (ppm)	Mn (ppm)	Ni (ppm)	Pb (ppm)	V (ppm)	Zn (ppm)
N11000	0	2	W-230139	3.83	301	.021	52	12	1.97	.02	392	18	12	50	42
N21000	0	2	W-232082	3.91	290	.025	50	10	2.03	.02	411	19	10	72	37
N41000	0	2	W-234559	3.62	288	.022	59	12	1.92	.01	459	31	14	58	45
N51000	0	2	W-236890	3.79	273	.020	57	14	1.96	.01	371	22	15	66	57
N61000	0	2	W-237758	3.41	294	.087	52	12	1.98	.01	342	20	16	76	42
N11100	0	2	W-230140	2.72	200	<.020	35	1.8	1.72	.01	235	5.0	8.8	32	30
N21100	0	2	W-232083	2.56	179	<.020	32	1.7	1.64	<.01	238	8.0	6.6	38	27
N11200	0	2	W-230141	3.49	268	.038	42	8.0	1.54	.02	256	11	12	42	32
N21200	0	2	W-232084	3.52	256	.063	41	5.6	1.54	.02	286	13	7.6	32	32
N41200	0	2	W-234560	3.16	233	<.020	40	5.3	1.56	.01	271	18	11	32	32
N51200	0	2	W-236891	3.55	235	.022	48	9.1	1.61	.00	273	18	13	55	38
N61200	0	2	W-237759	3.35	250	.098	46	8.3	1.69	.01	254	15	12	56	29
N11300	0	2	W-230142	4.88	384	.042	69	20	2.53	.02	419	37	12	82	61
N21300	0	2	W-232085	5.08	367	.046	70	18	2.74	.02	431	33	126?	91	65
N41300	0	2	W-234561	4.53	341	.055	72	16	2.37	.02	476	43	13	93	61
N51300	0	2	W-236892	4.67	324	.076	72	24	2.52	.02	474	34	20	93	77
N61300	0	2	W-237760	4.46	316	.060	69	20	2.61	.03	405	31	17	91	60
N11400	0	2	W-230143	3.60	278	.240	50	9.8	2.44	.02	422	23	11	75	43
N21400	0	2	W-232086	3.55	258	.022	49	11	2.35	.01	357	21	7.1	60	42
N11500	0	2	W-230144	3.30	279	.025	43	9.8	1.90	.02	383	19	11	58	38
N21500	0	2	W-232087	3.48	248	.046	47	10	2.25	.02	419	18	5.6	83	43
N41500	0	2	W-234562	5.09	318	.055	76	14	2.86	.02	340	52	16	103	63
N51500	0	2	W-236893	3.31	224	.029	56	14	2.06	.01	371	22	26	62	98
N61500	0	2	W-237761	5.28	375	.087	73	19	3.18	.02	417	39	13	120	70

Table 5. - Chemical analyses of the following size fractions of bottom sediment

[SO, undifferentiated; S1, >1,000 µm; S2, 1,000-5,000 µm; S3, 500-210 µm; S4, 210-105 µm; S5, 105-60 µm; S6, 60-30 µm; S7, 30-10 µm, S8, 10-1 µm; S9, <1 µm.]
Samples from stations 4 and 7. NO = blended samples from cruises 1, 2 and 3; 0-2 cm.

Field no.	Lab no.	Al (%)	Ba (ppm)	Cd (ppm)	Cr (ppm)	Cu (ppm)	Fe (%)	Hg (ppm)	Mn (ppm)	Ni (ppm)	Pb (ppm)	V (ppm)	Zn (ppm)
N0400S0	W-235210	2.63	209	.040	45	4.9	1.72	.06	259	24	16	44	32
N0400S1	W-235211	3.08	157	<.020	90	2.4	1.40	.06	209	53	8.7	31	22
N0400S2	W-235212	.72	118	.091	18	3.5	1.10	.06	289	15	10	23	15
N0400S3	W-235213	1.43	117	<.020	20	2.3	1.28	.04	107	5	6.7	20	20
N0400S4	W-235214	2.01	210	.029	33	3.4	1.19	.05	192	5	5.9	25	18
N0400S5	W-235215	2.38	254	.022	33	2.3	1.26	.06	244	5	12	34	23
N0400S6	W-235216	3.00	245	.096	80	6.5	1.69	.09	469	20	11	61	40
N0400S7	W-235217	3.82	266	.027	69	9.2	1.97	.07	467	16	9.6	74	47
N0400S8	W-235218	5.06	324	<.100	75	36.0	2.74	.20	489	24	31	79	80
N0400S9	W-235219	6.22	415	.462	88	36.7	4.14	.09	632	48	30	125	125
N0700S0	W-235220	1.65	142	.070	48	6.0	2.58	.05	171	8	7.9	38	28
N0700S1	W-235221	1.36	81	<.020	48	3.2	4.89	.05	53	8	5.0	45	35
N0700S2	W-235222	1.22	64	<.020	56	3.2	4.96	.05	57	7	28	45	37
N0700S3	W-235223	1.24	87	<.020	58	<2.0	4.18	.05	57	7	6.7	37	26
N0700S4	W-235224	1.13	154	.230	19	<2.0	1.01	.07	83	3	5.2	16	14
N0700S5	W-235225	2.32	220	.025	97	4.6	2.95	.06	932	13	16	100	63
N0700S6	W-235226	3.11	209	.140	82	6.0	2.21	.06	548	13	13	77	49
N0700S7	W-235227	4.23	272	.110	71	15	2.56	.05	387	25	20	87	66
N0700S8	W-235228	5.77	362	.310	96	30	3.84	.10	470	50	31	100	140
N0700S9	W-235229	6.46	321	.238	95	40	4.62	.15	541	54	48	151	140

Table 6. - Chemical analysis of the fine fraction from station blends. Size range of fine fraction: X = <60 µm, S7 = 10-30 µm.

Field no.	Top (cm)	Btm (cm)	Lab no.	Al (%)	Ba (ppm)	Cd (ppm)	Cr (ppm)	Cu (ppm)	Fe (%)	Hg (ppm)	Mn (ppm)	Ni (ppm)	Pb (ppm)	V (ppm)	Zn (ppm)
N10400X	0	2	W-230153	4.26	300	.048	70	15	2.61	.03	538	31	13	87	58
N20400X	0	2	W-232096	4.45	298	.063	64	18	2.83	.02	606	32	16	142	61
N30400X	0	2	W-232062	4.64	291	.091	69	15	2.77	.03	460	29	11	94	65
N40500X	0	2	W-234548	4.53	379	.025	74	19	2.66	.02	791	45	15	88	63
N40600X	0	2	W-234549	4.62	387	.038	76	20	2.68	.04	759	45	16	113	61
N50600S7	0	2	W-236904	4.37	303	.074	67	21	2.24	.04	809	32	23	90	62
N60600S7	0	2	W-237762	4.39	289	.071	67	14	2.22	.05	812	27	17	83	47
N10700X	0	2	W-230154	4.35	265	.120	83	21	2.80	.04	365	42	19	100	68
N20700X	0	2	W-232097	4.42	257	.088	74	19	3.40	.04	715	35	26	126	71
N30700X	0	2	W-232063	4.34	241	.150	68	19	2.71	.04	334	33	15	96	58
N10800X	0	2	W-230155	5.10	419	.075	72	22	2.89	.03	772	41	16	102	71
N20800X	0	2	W-232098	4.94	418	.037	68	22	2.85	.04	878	35	14	112	71
N30800X	0	2	W-232064	4.63	368	.120	63	23	2.67	.03	667	30	11	96	65
N40800X	0	2	W-234550	4.72	335	.055	73	18	2.56	.04	416	43	15	81	63
N50800S7	0	2	W-236905	5.09	368	.100	78	34	2.83	.04	836	45	26	110	86
N60800S7	0	2	W-237763	4.42	279	.039	65	13	2.29	.04	608	31	18	99	56
N40900X	0	2	W-234551	4.56	335	.055	76	18	2.55	.03	546	43	16	108	60
N41000X	0	2	W-234552	5.75	380	.066	90	20	3.24	.03	586	57	13	120	73

suggests that these sediments are not greatly contaminated, if at all, by industrial activity such as the exploratory drilling on Georges Bank.

Trace-metal variations with depth in sediments

Samples from eight stations, all from the first cruise, have been subsampled as a function of sediment depth to determine the depth profiles of metal concentrations. The metal concentrations are shown in Table 7 and selected metals are plotted in Figures 3 to 10.

At most stations, the Ba concentrations are either uniform with depth or increase slightly with increasing sediment depth. Cores 4 and 5 show the greatest increase in Ba concentration with sediment depth. The increase is probably related to texture. The concentration of silt plus clay increases over the same sediment depth interval (Table 8).

We used the concentration of Al as an index of the concentration of fine sediment (see Figure 2A and 2C) and calculated the Ba/Al ratio for sediment profiles. In addition to normalizing the trace-metal data for variations in texture, this procedure also corrects for variations in calcium carbonate and interstitial salt. The Ba/Al ratios at Stations 4, 5, 6, 7 and, to a lesser extent, Stations 10 and 15 have elevated values at the surface of the sediment compared to deeper sediment in the core. At some of these stations (4, 5, and 7), relatively high levels of Ba/Al ratio are constant to a sediment depth greater than 10 cm.

It is remotely possible that the Ba/Al elevations in surface sediments are related to the drilling-mud discharges that occurred on Georges Bank between July, 1981 and September, 1982. On the continental shelf adjacent to drilling locations, this ratio was up to 9 times higher in surface sediments than in sediments 12 cm below the sea floor (Bothner and others 1985b). The problems with this hypothesis in explaining enriched Ba/Al on the slope,

Table 7. - Chemical analyses of core samples subsectioned in 2-cm intervals.

Field no.	Top (cm)	Btm (cm)	Lab no.	Al (%)	Ba (ppm)	Cd (ppm)	Cr (ppm)	Cu (ppm)	Fe (%)	Hg (ppm)	Mn (ppm)	Ni (ppm)	Pb (ppm)	V (ppm)	Zn (ppm)
N10411	0	2	W-230145	2.69	239	<0.020	38	9.8	1.73	0.01	292	7.0	9.1	33	27
N10411	2	4	W-230156	2.70	233	.033	39	4.8	1.65	.01	232	6.0	9.1	36	28
N10411	4	6	W-230157	2.90	252	.038	41	5.0	1.75	.01	233	10	9.6	36	30
N10411	6	8	W-230158	3.00	245	.033	41	5.3	1.75	.01	243	12	8.8	42	30
N10411	8	10	W-230159	3.17	254	.055	44	6.1	1.86	.01	256	14	6.1	44	33
N10411	10	12	W-230160	3.08	247	.066	45	5.6	1.76	.01	250	11	7.1	47	33
N10411	12	14	W-230161	3.52	263	.058	49	7.5	2.01	.01	279	19	7.0	56	37
N10500	0	2	W-230134	2.52	248	.021	41	9.8	1.38	.01	395	15	8.8	30	27
N10511	2	4	W-230734	2.94	257	.028	43	11		.01	427	13	7.5	36	32
N10511	4	6	W-230735	2.96	266	.140	43	8.1	1.59	.01	394	9.5	6.1	31	29
N10511	6	8	W-230736	3.04	276	.038	46	8.8	1.62	.01	260	12	7.0	36	32
N10511	8	10	W-230737	3.08	270	.130	46	8.8	1.58	.01	239	13	7.1	33	32
N10511	10	12	W-230738	3.55	284	.100	50	9.3	1.78	.01	258	15	7.3	40	35
N10511	12	14	W-230739	4.24	322	.130	60	13	2.11	.01	306	20	8.3	56	44
N10511	14	16	W-230740	4.72	351	.095	67	16	2.43	.01	332	30	10	62	51
N10600	0	2	W-230135	3.21	307	.021	68	9.3	1.74	.02	491	16	8.0	59	35
N10611	2	4	W-230741	4.30	334	.085	62	13	2.22	.01	300	24	8.9	60	49
N10611	4	6	W-230742	4.08	326	.083	58	12	2.00	.01	280	20	7.3	62	40
N10611	6	8	W-230743	3.98	322	.095	60	12	2.02	.01	277	20	8.3	56	41
N10611	8	10	W-230744	3.93	321	.091	55	14	1.95	.01	268	18	8.8	69	42
N10611	10	12	W-230745	3.87	316	.075	55	13	1.95	.01	265	18	8.8	56	40
N10611	12	14	W-230746	3.76	312	.028	54	11	1.93	.01	321	17	6.3	53	40
N10611	14	16	W-230747	3.76	311	.038	55	11	1.94	.01	500	19	6.3	49	42
N10711	0	2	W-230150	2.09	174	.030	48	5.3	2.55	.01	211	8.0	11	33	30
N10711	2	4	W-230748	2.56	190	.100	58	7.1	2.27	.01	215	14	7.3	60	32
N10711	4	6	W-230749	2.77	199	.130	60	8.8	2.38	.01	200	15	8.3	62	36
N10711	6	8	W-230750	2.66	191	.095	61	8.8	2.45	.01	200	15	8.3	49	36
N10711	8	10	W-230751	2.92	195	.110	65	10	2.65	.01	199	18	10	66	39
N10711	10	12	W-230752	2.92	192	.095	63	11	2.53	.01	200	18	13	53	39
N10711	12	14	W-230753	3.18	188	.075	67	11	3.00	.01	182	24	12	66	43
N10711	14	16	W-230754	2.92	174	.075	68	8.8	3.21	.01	175	18	12	62	38
N10711	16	18	W-230755	2.67	190	.050	65	7.6	2.94	.01	175	16	10	53	36
N10831	0	2	W-232066	3.66	332	<.020	51	14	2.07	.03	536	22	10	72	40
N10831	2	4	W-232067	3.78	346	.037	50	18	2.13	.02	474	19	10	72	45
N10831	4	6	W-232068	3.68	342	.025	50	14	2.06	.02	275	19	9.1	49	40
N10831	6	8	W-232069	3.81	353	.037	53	15	2.12	.02	269	19	9.6	78	45
N10831	8	10	W-232070	3.54	333	.046	47	13	1.92	.02	251	19	7.6	74	40
N10831	10	12	W-232071	3.59	345	.056	50	14	1.96	.02	252	22	7.1	78	37
N10831	16	18	W-232072	3.78	351	.056	52	16	2.12	.01	262	26	7.1	54	45
N10831	22	24	W-232073	3.80	357	.042	50	15	2.15	.01	266	24	6.6	83	42
N10900	0	2	W-230138	4.72	359	.075	66	18	2.44	.02	343	32	12	83	58
N10931	2	4	W-230756	5.01	375	.120	72	18	2.50	.01	272	37	8.3	85	55
N10931	4	6	W-230757	4.89	370	.095	72	17	2.41	.01	260	34	8.3	80	60
N10931	6	8	W-230758	5.03	370	.110	74	19	2.49	.01	271	34	8.8	87	53
N10931	10	12	W-230759	5.04	372	.120	73	19	2.52	.01	269	35	8.8	82	57
N10931	14	16	W-230760	5.02	372	.120	73	20	2.47	.01	267	37	8.3	80	53
N10931	18	20	W-230761	4.94	375	.110	75	20	2.40	.01	265	34	9.5	71	55
N10931	22	24	W-230762	4.94	374	.110	69	17	2.38	.01	267	34	8.8	80	53
N10931	26	28	W-230763	4.96	359	.083	70	18	2.43	.02	302	34	11	85	56
N11000	0	2	W-230139	3.83	301	.021	52	12	1.97	.02	392	18	12	50	42
N11031	2	4	W-230764	4.52	340	.095	61	14	2.20	.01	253	27	7.0	76	52
N11031	4	6	W-230765	4.43	334	.083	63	13	2.12	<.01	254	24	7.0	71	47
N11031	6	8	W-230766	4.44	337	.075	63	13	2.13	.01	250	24	6.6	71	46
N11031	8	10	W-230767	4.27	325	.095	60	14	2.03	<.01	245	24	7.5	71	39
N11031	12	14	W-230768	4.14	323	.100	60	13	1.96	.01	239	20	9.5	66	42
N11031	16	18	W-230769	4.12	324	.083	58	13	1.96	.01	239	22	8.3	71	42
N11031	20	22	W-230770	3.86	313	.133	54	12	1.90	.01	254	18	9.1	62	42
N11500	0	2	W-230144	3.30	279	.025	43	9.8	1.90	.02	383	19	11	58	38
N11511	2	4	W-230719	2.08	139	<.020	26	6.5	1.12	<.01	135	9.0	3.8	23	21
N11511	4	6	W-230720	4.86	318	.058	62	14	2.62	.01	301	28	7.5	68	59
N11511	6	8	W-230721	4.40	297	.058	58	14	2.39	.01	271	26	7.6	68	51
N11511	8	10	W-230722	4.48	309	.091	60	15	2.43	.01	275	27	8.3	76	56
N11511	12	14	W-230723	4.02	301	.075	53	14	2.19	.01	249	23	8.3	66	49
N11511	16	18	W-230724	3.64	274	.027	50	11	2.09	.01	420	20	6.3	68	44

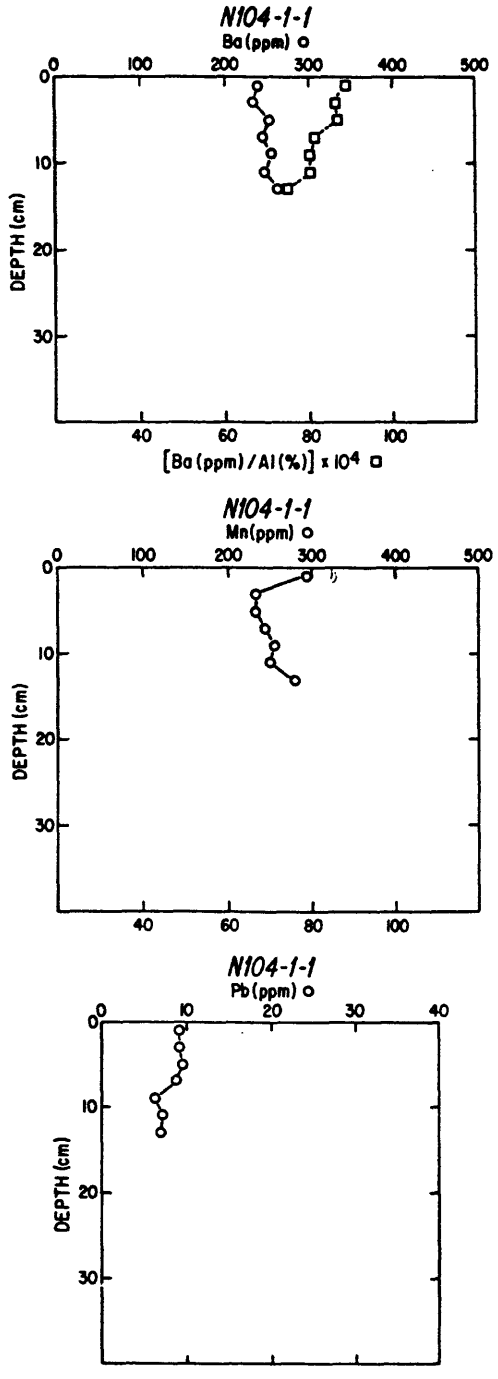

Figure 3. Distribution of barium, manganese, and lead with sediment depth at Station 4, Cruise 1.

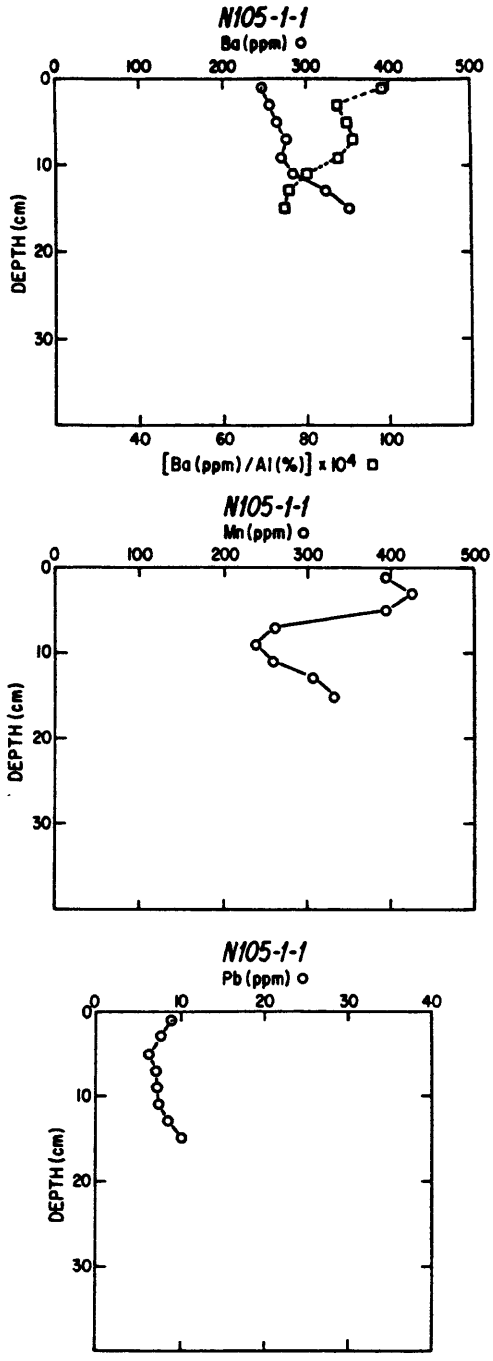

Figure 4. Distribution of barium, manganese, and lead with sediment depth at Station 5, Cruise 1.

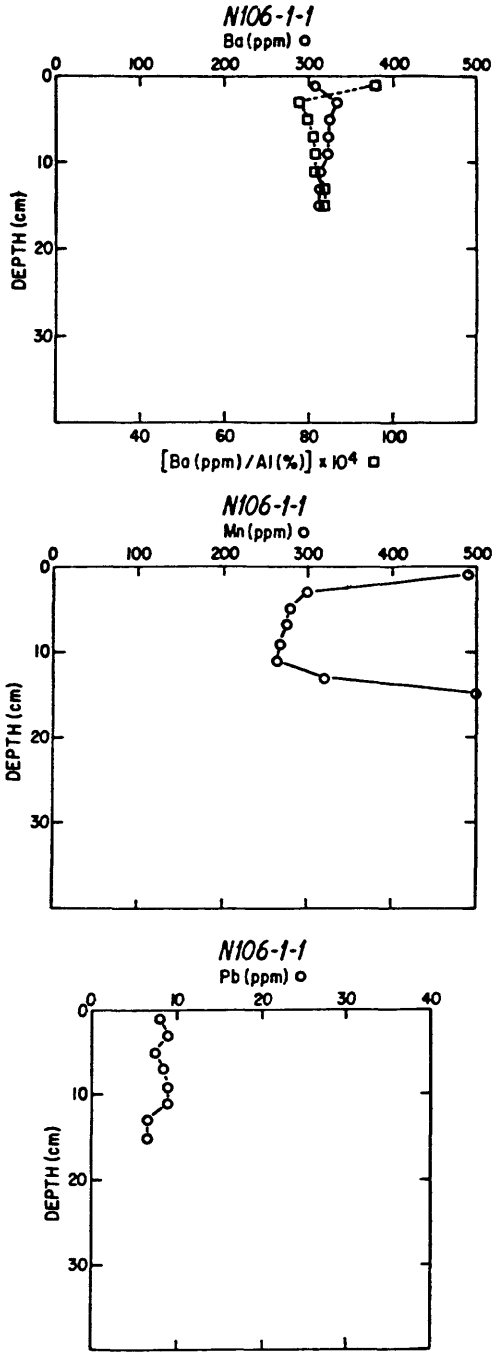

Figure 5. Distribution of barium, manganese and lead with sediment depth at Station 6, Cruise 1.

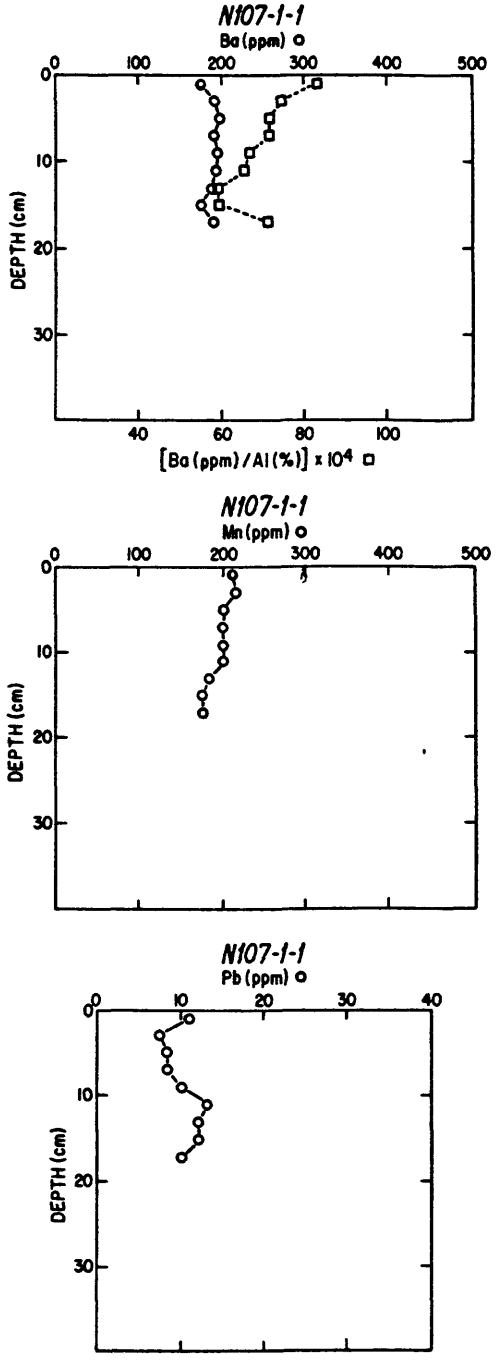

Figure 6. Distribution of barium, manganese, and lead with sediment depth at Station 7, Cruise 1.

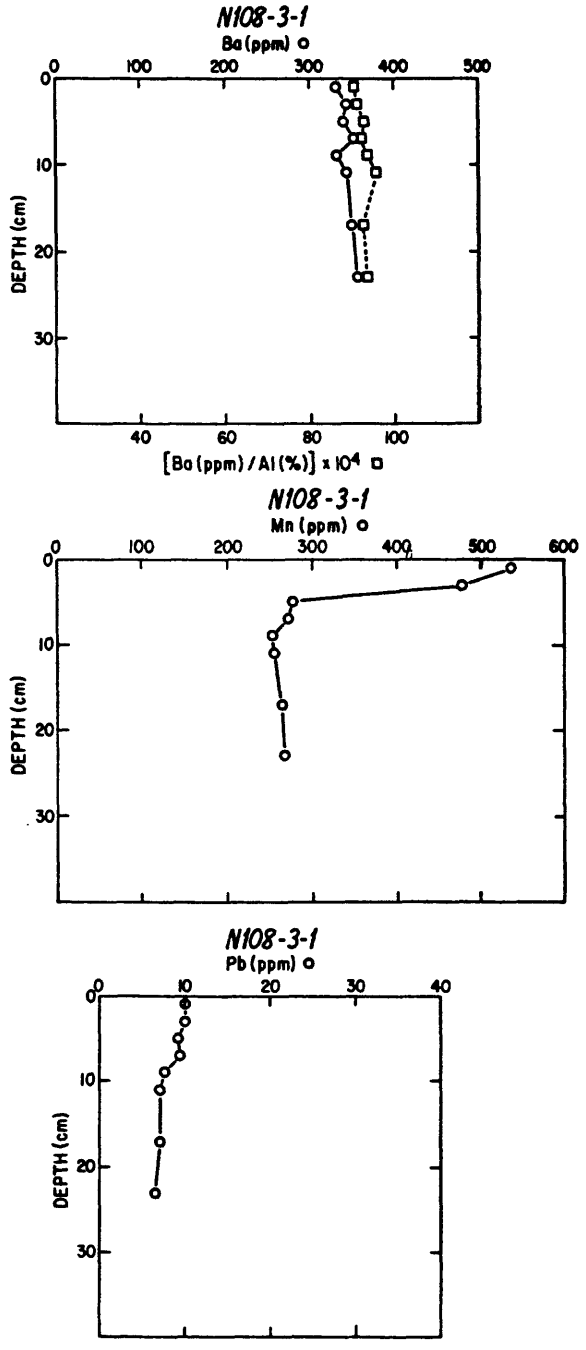

Figure 7. Distribution of barium, manganese, and lead with sediment depth at Station 8, Cruise 1.

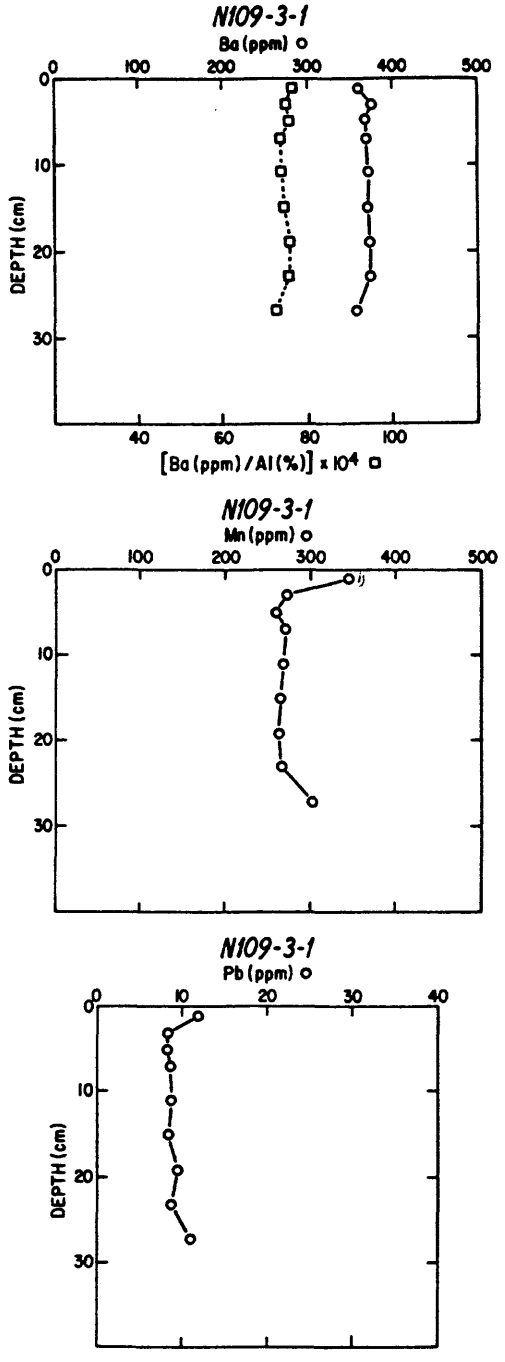

Figure 8. Distribution of barium, manganese, and lead with sediment depth at Station 9, Cruise 1.

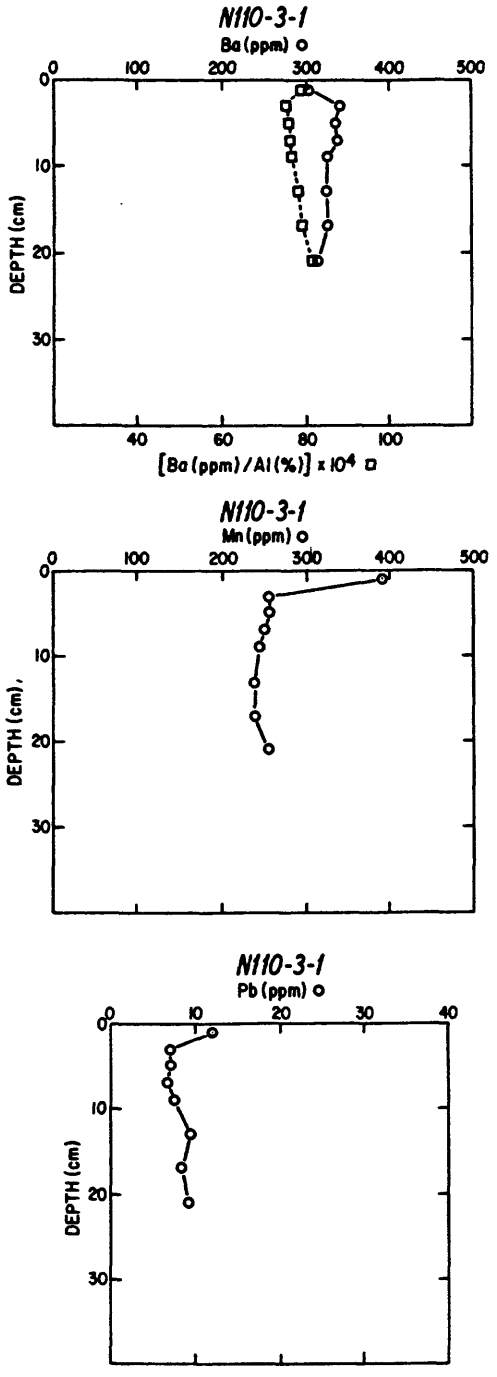

Figure 9. Distribution of barium, manganese, and lead with sediment depth at Station 10, Cruise 1.

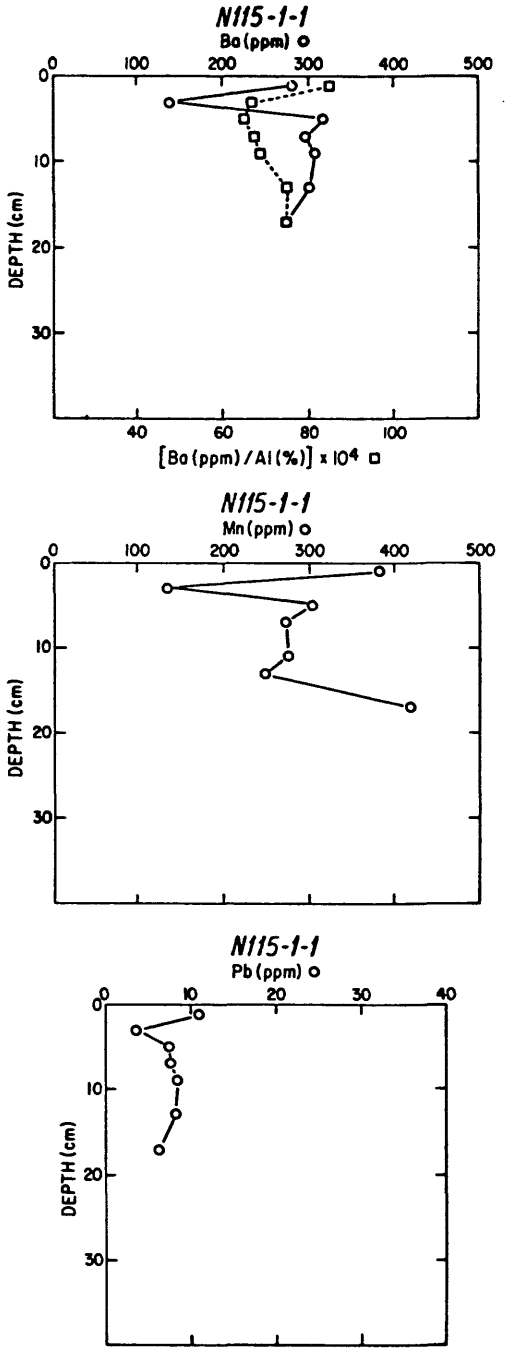

Figure 10. Distribution of barium, manganese, and lead with sediment depth at Station 15, Cruise 1.

Table 8. - Textural analyses of samples from depth intervals of box cores.

Core	Depth (cm)	% Gravel	% Sand	% Silt	% Clay
N104-1-1	0-2	4.1	61.2	14.6	20.1
	2-4	4.8	56.0	20.4	18.8
	4-6	1.7	57.2	19.3	21.8
	6-8	1.9	61.5	28.0	8.7
	8-10	0.9	58.6	26.4	14.1
	10-12	2.2	57.5	24.4	15.6
	12-14	0.0	54.0	28.1	17.9
N105-0-0	0-2	-	54.0	23.6	22.4
N105-1-1	2-4	-	44.2	32.2	23.7
	4-6	-	47.3	26.9	25.8
	6-8	-	42.4	28.9	28.6
	8-10	-	47.0	26.8	26.3
	10-12	-	41.6	31.0	27.4
	12-14	-	33.0	32.6	34.1
	14-16	-	25.6	32.9	41.6
N107-1-1	0-2	-	72.2	12.0	15.8
	2-4	-	64.7	18.0	17.3
	4-6	-	64.5	20.6	14.9
	6-8	-	61.4	21.8	16.8
	8-10	-	59.1	23.1	17.8
	10-12	-	53.5	26.3	20.3
	12-14	-	53.4	24.5	22.1
	14-16	-	63.1	18.0	18.9
	16-18	-	68.7	16.1	15.2
N115-0-0	0-2	-	34.0	33.0	33.0
N115-1-1	2-4	-	20.2	33.4	46.3
	4-6	-	25.3	31.7	43.0
	6-8	-	27.4	31.1	41.5
	8-10	2.9	23.2	34.8	39.2
	12-14		26.7	32.9	40.4
	16-18	-	34.4	29.9	35.7

however, are that the Ba is not enriched in the surface sediments and the sediment mixing rate would have to be high to account for enriched Ba/Al ratios at sediment depths greater than 10 cm during the 2.3 years that have lapsed since the end of drilling on the bank. Mixing rates have not been determined but should be estimated using profiles of ^{210}Pb, ^{137}Cs, and ^{234}Th.

The concentration of Mn is typically highest at the sediment surface and lower deeper in the core. This is common in sediments which undergo a transition from oxidizing conditions near the water/sediment interface to reducing conditions in deeper sediments. The profile is a result of MnO_2 dissolving under reducing conditions, diffusing upward, and precipitating in the oxidized environment near the surface (Lynn and Bonati, 1965). The deviations from this simple profile, as observed at Stations 5, 6, and 15, may be related to variability in texture or mineralogy.

The profiles of Pb with depth, particularly at stations 4, 6, and 8 (Figures 3, 5, and 7) are common in areas of fine sediment on the continental shelf and slope (Bothner and others, 1981; Bothner and others, 1985a). At these stations, the concentration of Pb in the upper 10 cm of sediment is 20%-33% higher than the concentration in sediments deeper than 10 cm. However, the highest concentration measured in bulk surface sediments from this area is only 18 ppm, which is less than the value in world average shales (20 ppm; see Krauskopf, 1967). For additional perspective, the average concentration of Pb in bulk surface sediments of Boston Harbor is 145 ppm (M. H. Bothner, 1985, unpublished data on file in Woods Hole, Mass.).

The elevated Pb concentrations in surficial sediments in this study area are thought to be related to an increased supply of Pb to these sediments, probably from the burning of Pb alkyls in gasoline in coastal metropolitan areas. The changes in lead inputs to the ocean attributable to this source

have been documented by the analysis of total and isotopic Pb in the annual growth bands of corals growing around Bermuda, (Shen, 1986). The use of Pb alkyls began in 1924 and has increased each year since 1940 until the recent switch to unleaded gasoline. The penetration of Pb to a depth of about 10 cm is possibly related to biological reworking of the sediment.

The impact of this increase in Pb is unknown. Important questions are: How is the Pb bound in the sediments? What is the bioavailability of this Pb? What is the response of organisms at different life stages to long-term, low level Pb contamination? Although a few studies show a relationship between the concentration of Pb in the tissue of deposit feeding organisms and the Pb concentration in acid-leached sediment (Luoma and Bryan, 1978; Tessier and others, 1984), no guidelines for safe levels of Pb in sediments have been established. Work addressing this complex issue is presently funded by the Environmental Protection Agency.

Although the large-scale processes of atmospheric and oceanic circulation might distribute urban-derived Pb homogeneously within the study area, localized processes such as sediment resuspension, winnowing, and mixing may result in differing Pb profiles at the stations sampled. The relative magnitude of the Pb enrichment and the nature of the Pb concentration gradient with depth may yield information about the occurrence and rates of such local processes.

Comparison between canyon and intercanyon

Station 7 in the axis of Lydonia Canyon and Station 4 on the adjacent slope, both at approximately 550-m water depth, provide an opportunity to compare these different physiographic environments with respect to trace-metal and sediment characteristics. These locations coincide with previous measurements of currents, turbidity, and resuspended sediment fluxes (using

sediment traps) made as part of the Lydonia Canyon Sediment Dynamics Experiment (Bothner and others, 1983, 1986; Butman and others, 1982a,b; Butman, 1983, 1986). These earlier studies showed that sediment resuspension in the axis of Lydonia Canyon was much higher (factor of 20-40) than at a station of comparable depth on the adjacent slope. It was also noted that ^{210}Pb and ^{137}Cs inventories determined during the Lydonia Canyon Experiment are higher in the sediments taken from the canyon axis than in those obtained on the open slope (Bothner and others, 1986).

One explanation for the higher isotope inventories in sediments from the canyon axis is that the higher flux of resuspended sediment, or more frequent resuspension, provides the fine-grained sediment more time and opportunity to adsorb metals from the water column (Bothner and others, 1986). If this preliminary hypothesis is correct, it may mean that deposit feeders and filter feeders living in the canyons might be more susceptible to contaminants added to the water column than those living on the open slope would be.

This hypothesis is supported by the metal-to-aluminum ratio in both bulk sample and the fine fraction analyzed during this program (Table 9). The ratios for Cd, Cr, Fe, and Pb to Al are consistently higher at Station 7 than at Station 4 for both the bulk and fine fraction samples. The clearest signal is the Pb/Al ratio, which on average is 64% higher at Station 7 than Station 4.

Higher values of Pb/Al ratios in bulk samples inside and outside of the canyon axis were also measured at 2200-m water depth. The mean (and standard deviation) of 5 replicates at Station 8, within the canyon axis, is 4.52±.85 and at Station 6, outside the canyon, the mean is 3.14±.54. The difference is significant at the 95% level of confidence. The Pb/Al ratio in a fine fraction (<60 μm) sample from Station 8 was also higher than the comparable

Table 9. Metal to Al% ratios for Stations 4, 6, 7, 8, 9, 10 from cruises 1-6. Samples include sediment blends, <60 µm size fraction and 10-30 µm size fraction.

Field no.	Lab no.	Fe/Al%	Ba/Al%	Cd/Al%	Cr/Al%	Cu/Al%	Hg/Al%	Mn/Al%	Ni/Al%	Pb/Al%	V/Al%	Zn/Al%
Sediment blends												
N10400	W-230133	.60	96.33	.01	15.92	2.57	.00	110.61	3.67	3.71	10.61	9.39
N20400	W-232076	.64	85.60	.01	13.58	2.06	.00	110.70	2.43	2.35	15.64	9.47
N30400	W-232050	.66	80.41	.01	14.69	2.29	.01	107.35	3.27	2.57	8.16	9.39
N30400	W-232065	.64	79.59	.01	15.10	2.65	.00	105.31	4.08	2.37	8.16	10.20
N10600	W-230135	.54	95.64	.01	21.18	2.90	.00	152.96	4.98	2.49	18.38	10.90
N20600	W-232078	.52	87.93	.01	12.69	2.97	.00	138.08	4.33	1.70	24.15	8.36
N40600	W-234556	.55	92.93	.01	14.47	3.15	.01	149.84	6.43	1.19	14.15	11.90
N50600	W-236887	.53	82.30	.01	14.43	4.59	.00	143.93	6.23	3.28	15.74	12.79
N60600	W-237755	.58	88.45	.01	15.84	4.29	.01	148.84	5.94	3.63	19.14	10.56
N10700	W-230136	1.28	90.76	.01	26.63	2.17	.00	111.96	2.72	4.95	25.54	13.59
N20700	W-232079	1.64	100.76	.02	26.72	.76	.00	123.66	1.53	4.20	11.45	.76
N30700	W-232052	1.54	77.78	.03	28.89	2.94	.01	121.11	3.89	4.89	12.22	13.89
N10800	W-230137	.57	86.67	.01	13.89	3.33	.01	136.67	5.28	3.06	14.44	11.67
N20800	W-232080	.57	93.97	.01	14.92	2.86	.01	145.08	5.08	2.41	15.56	11.11
N30800	W-232053	.58	96.15	.01	15.38	3.50	.01	128.32	4.20	2.62	13.99	11.19
N40800	W-234557	.59	139.05	.01	16.27	3.25	.00	113.91	8.28	1.30	15.09	11.24
N50800	W-236888	.56	87.13	.01	16.08	4.68	.00	130.99	5.85	4.39	18.13	19.88 ?
N60800	W-237756	.65	90.13	.01	15.88	3.43	.00	120.17	5.15	4.21	16.74	9.87
N10900	W-230138	.52	76.06	.02	13.98	3.81	.00	72.67	6.78	2.54	17.58	12.29
N20900	W-232081	.53	75.55	.01	13.44	3.08	.01	116.74	6.17	2.42	23.35	13.44
N40900	W-234558	.51	75.90	.02	16.22	4.28	.00	95.50	9.68	1.53	18.92	13.06
N50900	W-236889	.52	68.92	.03	15.01	4.86	.00	67.86	10.99	3.59	19.87	84.57 ?
N60900	W-237757	.57	71.50	.02	17.63	3.86	.01	87.44	7.49	3.62	22.22	15.22
N11000	W-230139	.51	78.59	.01	13.58	3.13	.00	102.35	4.70	3.13	13.05	10.97
N21000	W-232082	.52	74.17	.01	12.79	2.56	.01	105.12	4.86	2.56	18.41	9.46
N41000	W-234559	.53	79.56	.01	16.30	3.31	.00	126.80	8.56	1.60	16.02	12.43
N51000	W-236890	.52	72.03	.01	15.04	3.69	.00	97.89	5.80	3.96	17.41	15.04
N61000	W-237758	.58	86.22	.03	15.25	3.52	.00	100.29	5.87	4.69	22.29	12.32
<60µm Size Fraction												
N10400X	W-230153	.61	70.42	.01	16.43	3.52	.01	126.29	7.28	3.05	20.42	13.62
N20400X	W-232096	.64	66.97	.01	14.38	4.04	.00	136.18	7.19	3.60	31.91	13.71
N30400X	W-232062	.60	62.72	.02	14.87	3.23	.01	99.14	6.25	2.37	20.26	14.01
N40600X	W-234549	.58	83.77	.01	16.45	4.33	.01	164.29	9.74	1.36	24.46	13.20
N10700X	W-230154	.64	60.92	.03	19.08	4.83	.01	83.91	9.66	4.37	22.99	15.63
N20700X	W-232097	.77	58.14	.02	16.74	4.30	.01	161.76	7.92	5.88	28.51	16.06
N30700X	W-232063	.62	55.53	.03	15.67	4.38	.01	76.96	7.60	3.46	22.12	13.36

Table 9. - Continued Metal to Al% ratios for Stations 4, 6, 7, 8, 9, 10 from cruises 1-6. Samples include sediment blends, <60 µm size fraction and 10-30 µm size fraction.

Field no.	Lab no.	Fe/Al%	Ba/Al%	Cd/Al%	Cr/Al%	Cu/Al%	Hg/Al%	Mn/Al%	Ni/Al%	Pb/Al%	V/Al%	Zn/Al%
N10800X	W-230155	.57	82.16	.01	14.12	4.31	.01	151.37	8.04	3.14	20.00	13.92
N20800X	W-232098	.58	84.62	.01	13.77	4.45	.01	177.73	7.09	2.83	22.67	14.37
N30800X	W-232064	.58	79.48	.03	13.61	4.97	.01	144.06	6.48	2.38	20.73	14.04
N40800X	W-234550	.54	70.97	.01	15.47	3.81	.01	88.14	9.11	1.33	17.16	13.35
N40800X	W-234587	.55	69.77	.01	14.59	4.02	.00	86.26	9.09	1.54	17.55	12.90
N40900X	W-234551	.56	73.46	.01	16.67	3.95	.01	119.74	9.43	1.60	23.68	13.16
N41000X	W-234552	.56	66.09	.01	15.65	3.48	.01	101.91	9.91	1.27	20.87	12.70
30-10 µm Size Fraction												
N50600S7	W-236904	.51	69.34	.02	15.33	4.81	.01	185.13	7.32	5.26	20.59	14.19
N60600S7	W-237762	.51	65.83	.02	15.26	3.19	.01	184.97	6.15	3.87	18.91	10.71
N50800S7	W-236905	.56	72.30	.02	15.32	6.68	.01	164.24	8.84	5.11	21.61	16.90
N60800S7	W-237763	.52	63.12	.01	14.71	2.94	.01	137.56	7.01	4.07	22.40	12.67

sample from Station 6. The analysis of the sediment size fraction between 10-30 μm at both stations were similar (Table 6), suggesting that the Pb enrichment may be more pronounced in the size fraction finer than 10 μm. These results suggest that processes of enhanced scavenging are active along much of the canyon axis.

Comparison of gully and nongully

A detailed bathymetric and sidescan-sonar survey of the upper slope off Georges Bank reveals that the areas between the major canyons are highly dissected by gullies (Scanlon, 1982). Stations 9 (gully) and 10 (nongully) were selected to compare the characteristics of sediments inside and outside one of these features that are abundant on the U.S. Atlantic continental slope.

Long-term current records obtained at each of these stations (Butman, 1986; B. Butman, 1986, unpublished data on file at USGS, Woods Hole, MA) indicate that the currents are slightly stronger at Station 10 than at 9. Outside of the gully (Station 10), mean speeds were 8.4±4.2 cm/sec, reaching speeds greater than 20 cm/sec 8 percent of the time. Inside of the gully (Station 9), mean speeds were 5.4±2.9 cm/sec with speeds greater than 20 cm/sec about 1% of the time. The transmissometer records show no measurable differences between sites and very little sediment resuspension.

Differences in sediment parameters are consistent with differences in currents. Sediments are slightly finer in the gully where the mean grain size is fine silt (7.3 φ) with 37 % clay. At Station 10, the sediments are a medium silt (6 φ) with 25 % clay (Battelle and others, 1985).

The trace-metal concentrations in bulk sediments (means of five surface samples, Table 4) are on average 43 % greater in the gully than outside the gully, probably related to the finer sediment. We examined the Pb/Al ratios

in samples from Stations 9 and 10 and found inconsistent results. The Pb/Al ratios for the bulk samples are higher at Station 10 (Table 9). In the fine fraction samples, the Pb/Al ratios are higher at Station 9. In contrast, the Pb/Al ratios in both bulk and fine-fraction samples from the canyon axis (Station 7) were higher than those from comparable depth on the adjacent slope. A possible cause for the consistently greater Pb/Al enrichment in the canyon axis is the much greater flux of resuspended sediment (Bothner and others, 1986).

SUMMARY OF MAJOR FINDINGS

1. There is evidence in this data set which supports the hypothesis that the fine sediments in the axis of Lydonia Canyon are more effective scavengers of trace metals from the water column than are sediments on the adjacent slope at comparable water depths. The mechanism for this enhanced scavenging is thought to be the increased resuspension of bottom sediments, as documented in a previous study (Bothner and others, 1986; Butman, 1986). We found that the metal-to-aluminum ratios for Cd, Cr, Cu, and Pb in both the fine fraction and bulk sample were higher at Station 7 (canyon axis) than at Station 4 (slope).

   If correct, this hypothesis would imply that filter feeders and deposit feeders living in the canyon axis might be more susceptible to wastes discharged to the water column than organisms living at comparable depths on the slope.

2. The upper slope between the major canyons in this study area is highly dissected by small topographic features referred to as gullies. In comparing the sediment chemistry inside and outside a gully, we found higher concentrations of metals (typically 20% to 50% higher) in the

gully. This difference may be solely dependent on the higher concentrations of clay-sized sediment (average of 38% higher) within the gully. Current and textural data suggest that the gully (Station 9) is a more quiescent depositional environment than the intergully area (Station 10).

3. The concentrations of metals at the slope stations of this program are lower than published average values for shales and modern clays (e.g. Krauskopf, 1967). This usually suggests that the sediments are not highly contaminated. There are generally higher concentrations of Pb in the surface sediments (about 30% higher) than in sediments deeper in the cores. The maximum concentration of Pb in bulk surface sediments from this study area is 18 ppm, lower than the concentration in average world shales (20 ppm, Krauskopf, 1967). Similar Pb profiles have been previously described in sediments from other locations off the U.S. East Coast (Bothner and others, 1981; Bothner and others, 1985a). The enrichment is thought to be related to the burning of gasoline containing Pb additives and its subsequent atmospheric transport to offshore marine areas.

REFERENCES

Battelle New England Marine Research Laboratory, Woods Hole Oceanographic Institution, and Lamont-Doherty Geological Observatory, 1986, Study of biological processes on the U.S. North Atlantic Slope and Rise: Interim Report submitted to the U.S. Minerals Management Service under Contract No. 14-12-0001-30064, 201 p.

Bothner, M. H., Campbell, E. Y., DiLisio, G. P., Parmenter, C. M., Rendigs, R. R., Doughten, M. W., Johnson, R. G., Gillison, J. R., and Rait, N., 1985a, Analysis of trace metals in bottom sediments in support of deepwater biological processes studies on the U.S. Mid-Atlantic Continental Slope and Rise: Second Interim Report submitted to the U.S. Minerals Management Service under Interagency Agreement No. 14-12-0001-30197, 55 p.

Bothner, M. H., Parmenter, C. M., Rendigs, R. R., and Rubin, Meyer, 1986, The flux and composition of resuspended sediment in submarine canyons off the Northeastern United States: Implications for pollutant and scavenging: Chapter 6, in Butman, B., ed., North Atlantic Slope and Canyon Study: Final Report submitted to the U.S. Minerals Management Service under Interagency Agreement 14-12-0001-30180, 62 p.

Bothner, M. H., Parmenter, C. M., and Butman, 1983, Resuspended sediment flux in Lydonia and Oceanographer Canyons off the eastern United States (abs.): EOS, Transactions, American Geophysical Union, v. 64, no. 52, p. 1051.

Bothner, M. H., Rendigs, R. R., Campbell, Esma, Doughten, M. W., Parmenter, C. M., O'Dell, C. H., DiLisio, G. P., Johnson, R. G., Gillison, J. R., and Rait, Norma, 1985b, The Georges Bank monitoring program: Analysis of trace metals in bottom sediments during the third year of monitoring: Final report submitted to the U.S. Minerals Management Service under Interagency Agreement No. 14-12-0001-30153, 99 p.

Bothner, M. H., Spiker, E. C., Johnson, P. P., Rendigs, R. R., and Aruscavage P. J., 1981, Geochemical evidence for modern sediment accumulation on the Continental Shelf off southern New England: Journal of Sedimentary Petrology, v. 51, no. 1, p. 281-292.

Butman, B., 1983, Long-term current measurements in Lydonia and Oceanographer Canyons (abs.): EOS, Transactions, American Geophysical Union, v. 64, p. 1050.

Butman, B., 1985, Progress Report, North Atlantic Slope and Canyon Study: Progress report submitted to the U.S. Minerals Management Service under Interagency Agreement No. 14-12-0001-30180, 31 p.

Butman, B., 1986, Downslope flow associated with high-frequency current fluctuations observed on the outer continental shelf and upper slope along the Northeastern United States continental margin: Implications for sediment transport: Chapter 7 in Butman, B., ed., North Atlantic Slope and Canyon Study; Final Report submitted to the U.S. Minerals Management Service under Interagency Agreement 14-12-0001-30180, 53 p.

Butman, B., Bothner, M. H., Noble, M. A., and Twichell, D. C., 1982a, The Lydonia Canyon Experiment: Preliminary results (abs.): EOS, Transactions, American Geophysical Union, v. 63, p. 349.

Butman, B., Noble, M., Moody, J., and Bothner, B., 1982b, The Lydonia Canyon Dynamics Experiment Progress Report: Progress report submitted to the U.S. Minerals Management Service under Interagency Agreement AA851-IA2-66, 91 p.

Krauskopf, K. B., 1967, Introduction to geochemistry: New York, McGraw-Hill, 721 p.

Luoma, S. N., and Bryan, G. W., 1978, Factors controlling the availability of sediment-bound lead to the estuarine bivalve Scrobicularia plana: Journal of Marine Biological Association, v. 58, p. 793-802.

Lynn, D. C., and Bonati, E., 1965, Mobility of manganese in diagenesis of deep-sea sediments: Marine Geology, v. 3, p. 457-474.

Lyons, W. B. and Fitzgerald, W. F., 1983, Trace metals speciation in nearshore anoxic and suboxic pore waters, In Wong, C. S., eds., and others, Trace Metals in Sea Water: New York, Plenum Press, p. 621-641.

McCullough, J. R., Irwin, B. J., and Bowles, R. M., 1982, LORAN-C latitude-longitude conversion at sea: programming considerations: The Wild Goose Association, Annual Technical Symposium, 11th, Proceedings, p. 42-75.

McCullough, J. R., Irwin, B. J., Hayward, R. C., and Bowles, R. M., 1983, A first look at LORAN-C calibration data in the Gulf of Mexico: The Wild Goose Association, Annual Technical Symposium, 12th, Proceedings, p. 25-67.

Scanlon, K. M., 1982, Geomorphic features of the western North Atlantic Continental Slope between Northeast Channel and Alvin Canyon as interpreted from GLORIA II long-range sidescan-sonar data: U.S. Geological Survey Open-File Report 82-728, 10 p., 1 map sheet.

Shen, G. T., 1986, Lead and cadmium geochemistry of corals: Reconstruction of historic perturbations in the upper ocean: Ph.D. Dissertation, Joint Program in Oceanography and Oceanographic Engineering, Woods Hole Oceanographic Institution, Woods Hole, MA. Technical Report WHOI-86-37, 233 p.

Tessier, A., Campbell, P. G. C., Auclair, J. C., and Bisson, M., 1984, Relationships between the partitioning of trace metals in sediments and their accumulation in the tissues of the freshwater mollusc Elliptio complanta in a mining area: Canadian Journal of Fishieries and Aquatic Science, v. 41, p. 1463-1472.

Valentine, P. C., Uzmann, J. R., and Cooper R. A., 1980, Geology and biology of Oceanographer Submarine Canyon: Marine Geology, v. 38, p. 283-312.

Appendix table 1. Navigation data for stations analyzed for chemistry. Values corrected for additional secondary factors (asf), (McCullough and others, 1983).
[Time delay 1 (Caribou, Maine) and time delay 2 (Carolina Beach, N.C.) are Loran-C time delay values for the 9960 Loran-C chain].

Field Number	Station	Collection date (Yr Mo Dy)	Water depth (m)	Time delay 1 (μ seconds)	Time delay 2 (μ seconds)	Latitude (degrees) (and minutes)	Longitude (degrees) (and minutes)
N10100	01	1984 11 8	545	13016.8	43518.7	41 0.6568	-66 23.5290
N10200	02	1984 11 8	2103	13005.8	43495.1	40 57.1570	-66 13.5137
N20200	02	1985 4 26	2100	13005.9	43495.1	40 57.1542	-66 13.5383
N30200	02	1985 7 3	2099	13005.7	43495.4	40 57.2119	-66 13.5526
N40200	02	1985 11 23	2111	13005.7	43495.5	40 57.2294	-66 13.5738
N50200	02	1986 04 28	2104	13005.7	43495.1	40 57.1557	-66 13.4788
N60200	02	1986 07 25	2101	13005.7	43495.6	40 57.2398	-66 13.5850
N10300	03	1984 11 9	1344	13010.6	43520.1	41 1.3541	-66 19.9610
N20300	03	1985 4 26	1342	13010.9	43519.9	41 1.3111	-66 19.9913
N30300	03	1985 7 3	1332	13010.6	43520.2	41 1.3714	-66 19.9819
N40300	03	1985 11 22	1336	13010.7	43520.4	41 1.4059	-66 20.0237
N50300	03	1986 04 27	1344	13010.7	43520.5	41 1.4169	-66 20.0689
N60300	03	1986 07 25	1349	13010.1	43520.4	41 1.4263	-66 19.9049
N10400	04	1984 11 4	556	13461.5	43342.6	40 21.1983	-67 32.0730
N10400	04	1984 11 4	556	13461.5	43342.6	40 21.1983	-67 32.0730
N20400	04	1985 4 28	556	13461.5	43342.5	40 21.1822	-67 32.0580
N30400	04	1985 7 6	548	13461.3	43342.6	40 21.2020	-67 32.0287
N10500	05	1984 11 5	1317	13512.6	43249.1	40 5.1373	-67 29.6887
N20500	05	1985 4 29	2063	13512.6	43248.7	40 5.0718	-67 29.6302
N30500	05	1985 7 4	2061	13512.8	43243.8	40 4.2665	-67 28.9585
N40500	05	1985 11 25	2072	13512.7	43248.7	40 4.8223	-67 29.1894
N50500	05	1986 04 29	2070	13513.1	43248.7	40 5.0571	-67 29.7424
N60500	05	1986 07 26	2065	13512.7	43248.7	40 5.0660	-67 29.6371
N10600	06	1984 11 5	2113	13509.9	43248.4	40 5.0601	-67 28.9671
N20600	06	1985 4 29	2108	13509.8	43248.3	40 5.0451	-67 28.9295
N40600	06	1985 11 25	2114	13510.1	43248.4	40 4.8089	-67 28.5486
N50600	06	1986 04 30	2113	13510.1	43248.4	40 5.0519	-67 28.9968
N60600	06	1986 07 26	2112	13509.5	43248.3	40 5.0520	-67 28.8634
N10700	07	1984 11 10	560	13470.9	43382.8	40 27.4835	-67 40.0873
N20700	07	1985 4 28	559	13470.9	43382.8	40 27.4835	-67 40.0873
N30700	07	1985 7 6	557	13470.9	43382.9	40 27.4996	-67 40.1022
N10800	08	1984 11 11	2178	13524.4	43281.8	40 10.2863	-67 37.1113
N20800	08	1985 4 29	2183	13524.2	43281.7	40 10.2732	-67 37.0521
N30800	08	1985 7 5	2180	13524.3	43281.7	40 10.2717	-67 37.0745

Appendix table 1 - Continued

Field Number	Station	Collection date (Yr Mo Dy)	Water depth (m)	Time delay 1 (μ seconds)	Time delay 2 (μ seconds)	Latitude (degrees) (and minutes)	Longitude (degrees) (and minutes)
N40800	08	1985 11 25	2182	13524.8	43281.6	40 10.0041	-67 36.7173
N60800	08	1986 07 27	2191	13524.5	43281.6	40 10.2593	-67 37.1075
N10900	09	1984 11 12	1224	14263.1	43213.3	39 50.4364	-70 1.5533
N20900	09	1985 5 3	1228	14262.8	43213.3	39 50.4397	-70 1.4955
N40900	09	1985 11 27	1229	14262.9	43213.2	39 50.4251	-70 1.5072
N50900	09	1986 05 03	1220	14263.0	43213.6	39 50.4737	-70 1.5540
N60900	09	1986 07 28	1228	14263.1	43213.2	39 50.4258	-70 1.5548
N11000	10	1984 11 13	1223	14287.4	43197.9	39 48.1064	-70 5.0893
N21000	10	1985 5 3	1211	14287.4	43198.1	39 48.1332	-70 5.1041
N41000	10	1985 11 27	1225	14287.9	43197.9	39 48.1012	-70 5.1859
N51000	10	1986 05 03	1249	14288.4	43197.8	39 48.0852	-70 5.2661
N61000	10	1986 07 28	1236	14287.8	43197.8	39 48.0953	-70 5.1621
N11100	11	1984 12 8	254	14511.6	43321.1	40 1.2811	-70 55.0097
N21100	11	1985 5 4	250	14511.8	43321.2	40 1.2908	-70 55.0517
N11200	12	1984 11 15	556	14529.2	43267.2	39 54.3112	-70 55.0457
N21200	12	1985 5 4	553	14529.0	43267.1	39 54.3011	-70 55.0032
N41200	12	1985 11 30	554	14529.4	43267.2	39 54.3087	-70 55.0824
N51200	12	1986 05 06	553	14529.6	43266.8	39 54.2561	-70 55.1028
N61200	12	1986 07 30	562	14529.2	43266.8	39 54.2621	-70 55.0256
N11300	13	1984 12 9	1248	14542.5	43221.3	39 48.4219	-70 54.8654
N21300	13	1985 5 5	1247	14542.5	43220.9	39 48.3719	-70 54.8426
N41300	13	1985 11 29	1246	14542.8	43220.9	39 48.3687	-70 54.8984
N51300	13	1986 05 06	1252	14543.6	43219.4	39 48.1750	-70 54.9590
N61300	13	1986 07 30	1255	14542.6	43220.8	39 48.3520	-70 54.8673
N11400	14	1984 12 9	2107	14556.6	43161.9	39 40.8571	-70 54.1679
N21400	14	1985 5 5	2094	14556.4	43162.5	39 40.9339	-70 54.1634
N11500	15	1984 12 9	2155	14558.4	43155.6	39 40.0534	-70 54.1587
N21500	15	1985 5 5	2145	14558.6	43155.9	39 40.0893	-70 54.2134
N41500	15	1985 11 28	2141	14558.6	43155.6	39 40.0518	-70 54.1967
N51500	15	1986 05 05	2162	14558.7	43155.2	39 40.0063	-70 54.1862
N61500	15	1986 07 30	2156	14558.5	43155.8	39 40.0763	-70 54.1820
Navigation data (asf corrected) for replicate box core and within box core comparisons							
N10411	04	1984 11 4	565	13461.6	43342.6	40 21.1965	-67 32.0952
N10421	04	1984 11 4	572	13461.6	43342.7	40 21.2127	-67 32.1102
N10431	04	1984 11 5	530	13461.4	43342.6	40 21.2001	-67 32.0509
N10432	04	1984 11 5	530	13461.4	43342.6	40 21.2001	-67 32.0509
N10433	04	1984 11 5	530	13461.4	43342.6	40 21.2001	-67 32.0509

Appendix table 1 - Continued

Field Number	Station	Collection date (Yr Mo Dy)	Water depth (m)	Time delay 1 (μ seconds)	Time delay 2 (μ seconds)	Latitude (degrees) (and minutes)	Longitude (degrees) (and minutes)
Navigation for fine fraction samples							
N10400X	04	1984 11 4	556	13461.5	43342.6	40 21.1983	-67 32.0730
N20400X	04	1985 4 28	556	13461.5	43342.5	40 21.1822	-67 32.0580
N30400X	04	1985 7 6	548	13461.3	43342.6	40 21.2020	-67 32.0287
N40500X	05	1985 11 25	2072	13512.7	43248.7	40 4.8223	-67 29.1894
N40600X	06	1985 11 25	2114	13510.1	43248.4	40 4.8089	-67 28.5486
N50600S7	06	1986 04 30	2113	13510.1	43248.4	40 5.0519	-67 28.9968
N10700X	07	1984 11 10	560	13470.9	43382.8	40 27.4835	-67 40.0873
N20700X	07	1985 4 28	559	13470.9	43382.8	40 27.4835	-67 40.0873
N30700X	07	1985 7 6	557	13470.9	43382.9	40 27.4996	-67 40.1022
N10800X	08	1984 11 11	2178	13524.4	43281.8	40 10.2863	-67 37.1113
N20800X	08	1985 4 29	2183	13524.2	43281.7	40 10.2732	-67 37.0521
N30800X	08	1985 7 5	2180	13524.3	43281.7	40 10.2717	-67 37.0745
N40800X	08	1985 11 25	2182	13524.8	43281.6	40 10.0041	-67 36.7173
N50800S7	08	1986 04 29	2151	13525.1	43281.6	40 10.2232	-67 37.2284
N40900X	09	1985 11 27	1229	14262.9	43213.2	39 50.4251	-70 1.5072
N41000X	10	1985 11 27	1225	14287.9	43197.9	39 48.1012	-70 5.1859
Target Locations for Size Fractionation Analyses Prepared From Cruise Blends							
N00400S-	04	----------		13512.8	43248.8	40 05.0800	-67 29.86
N00700S-	07	----------		13470.9	43382.9	40 27.4800	-67 40.24

Appendix table 1 - Continued

Field Number	Station	Collection date (Yr Mo Dy)	Water depth (m)	Time delay 1 (μ seconds)	Time delay 2 (μ seconds)	Latitude (degrees) (and minutes)	Longitude (degrees) (and minutes)
N20411	04	1985 4 28	590	13461.9	43342.3	40 21.1425	-67 32.1166
N20412	04	1985 4 28	1340	13461.9	43342.3	40 21.1425	-67 32.1166
N20413	04	1985 4 28	1340	13461.9	43342.3	40 21.1425	-67 32.1166
N20421	04	1985 4 28	540	13461.5	43342.5	40 21.1821	-67 32.0580
N20431	04	1985 4 28	539	13461.4	43342.6	40 21.2002	-67 32.0508
N30411	04	1985 7 6	540	13461.3	43342.6	40 21.2020	-67 32.0287
N30412	04	1985 7 6	540	13461.3	43342.6	40 21.2020	-67 32.0287
N30413	04	1985 7 6	540	13461.3	43342.6	40 21.2020	-67 32.0287
N30421	04	1985 7 6	560	13461.3	43342.6	40 21.2020	-67 32.0287
N30431	04	1985 7 6	545	13461.4	43342.6	40 21.2001	-67 32.0509
N50611	06	1986 04 30	2120	13510.4	43247.8	40 4.9467	-67 28.9945
N50612	06	1986 04 30	2120	13510.4	43247.8	40 4.9467	-67 28.9945
N50613	06	1986 04 30	2120	13510.4	43247.8	40 4.9467	-67 28.9945
N50621	06	1986 04 30	2110	13510.0	43248.7	40 5.1132	-67 29.0450
N50631	06	1986 05 01	2109	13509.7	43248.6	40 5.0956	-67 28.9506
N10711	07	1984 11 10	560	13470.9	43382.9	40 27.4996	-67 40.1022
N10721	07	1984 11 10	560	13470.7	43382.6	40 27.4555	-67 40.0145
N10731	07	1984 11 10	560	13471.0	43382.8	40 27.4816	-67 40.1090
N20711	07	1985 4 28	560	13470.9	43382.9	40 27.4996	-67 40.1022
N20721	07	1985 4 28	560	13470.9	43382.8	40 27.4835	-67 40.0873
N20731	07	1985 4 28	540	13470.9	43382.6	40 27.4515	-67 40.0577
N30711	07	1985 7 6	556	13471.0	43382.8	40 27.4816	-67 40.1090
N30721	07	1985 7 6	555	13470.8	43383.0	40 27.5176	-67 40.0954
N30731	07	1985 7 7	560	13470.8	43382.8	40 27.4855	-67 40.0657
N50811	08	1986 04 29	2147	13524.9	43282.0	40 10.3108	-67 37.2396
N50812	08	1986 04 29	2147	13524.9	43282.0	40 10.3108	-67 37.2396
N50813	08	1986 04 29	2147	13524.9	43282.0	40 10.3108	-67 37.2396
N50821	08	1986 04 29	2165	13524.9	43281.4	40 10.2074	-67 37.1568
N50831	08	1986 04 29	2130	13525.7	43281.1	40 10.1517	-67 37.2891
Navigation (asf corrected) for profile sample							
N10411	04	1984 11 4	565	13461.6	43342.6	40 21.1965	-67 32.0952
N10511	05	1984 11 5	2065	13512.9	43249.0	40 5.1167	-67 29.7428
N10611	06	1984 11 5	2117	13509.8	43248.2	40 5.0287	-67 28.9148
N10711	07	1984 11 10	560	13470.9	43382.9	40 27.4996	-67 40.1022
N10831	08	1984 11 11	2180	13524.8	43281.7	40 10.2640	-67 37.1865
N10931	09	1984 11 12	1225	14262.6	43213.80	39 50.5092	-70 1.4948
N11031	10	1984 11 15	1235	14287.1	43197.5	39 48.0559	-70 5.0018
N11511	15	1984 12 9	2155	14558.4	43155.7	39 40.0659	-70 54.1643